HHS Public Access

Author manuscript

Cell Rep. Author manuscript; available in PMC 2024 July 10.

Published in final edited form as:

Cell Rep. 2024 May 28; 43(5): 114257. doi:10.1016/j.celrep.2024.114257.

Compensation between FOXP transcription factors maintains proper striatal function

Newaz I. Ahmed[1,2], **Nitin Khandelwal**[1,2], **Ashley G. Anderson**[1,3,4], **Emily Oh**[1,2], **Rachael M. Vollmer**[1,2], **Ashwinikumar Kulkarni**[1,2], **Jay R. Gibson**[1,2], **Genevieve Konopka**[1,2,5,*]

[1]Department of Neuroscience, UT Southwestern Medical Center, Dallas, TX 75390-9111, USA

[2]Peter O'Donnell Jr. Brain Institute, UT Southwestern Medical Center, Dallas, TX 75390-9111, USA

[3]Department of Molecular and Human Genetics, Baylor College of Medicine, Houston, TX 77030, USA

[4]Jan and Dan Duncan Neurological Research Institute at Texas Children's Hospital, Houston, TX 77030, USA

[5]Lead contact

SUMMARY

Spiny projection neurons (SPNs) of the striatum are critical in integrating neurochemical information to coordinate motor and reward-based behavior. Mutations in the regulatory transcription factors expressed in SPNs can result in neurodevelopmental disorders (NDDs). Paralogous transcription factors *Foxp1* and *Foxp2*, which are both expressed in the dopamine receptor 1 (D1) expressing SPNs, are known to have variants implicated in NDDs. Utilizing mice with a D1-SPN-specific loss of *Foxp1*, *Foxp2*, or both and a combination of behavior, electrophysiology, and cell-type-specific genomic analysis, loss of both genes results in impaired motor and social behavior as well as increased firing of the D1-SPNs. Differential gene expression analysis implicates genes involved in autism risk, electrophysiological properties, and neuronal development and function. Viral-mediated re-expression of *Foxp1* into the double knockouts is sufficient to restore electrophysiological and behavioral deficits. These data indicate complementary roles between *Foxp1* and *Foxp2* in the D1-SPNs.

In brief

*Correspondence: genevieve.konopka@utsouthwestern.edu.

AUTHOR CONTRIBUTIONS

N.I.A. and G.K. designed the study and wrote the paper. N.I.A. performed snRNA and ATAC-seq experiments, mouse behavior experiments, and contributed to immunohistochemistry (IHC) experiments. A.G.A. contributed to initial study design and aided in snRNA-seq experiments. E.O. and R.M.V. contributed to IHC experiments. J.G. and N.K. designed the electrophysiology experiments and aided in writing the paper. N.K. performed electrophysiology experiments and neonatal AAV injections. N.K. and N.I.A. performed FACS and qPCR experiments. A.K. performed pre-processing and analysis of all snRNA and ATAC-seq data.

DECLARATION OF INTERESTS

The authors declare no competing interests.

SUPPLEMENTAL INFORMATION

Supplemental information can be found online at https://doi.org/10.1016/j.celrep.2024.114257.

Ahmed et al. show in mice that transcription factors Foxp1 and Foxp2 compensate for each other to maintain proper striatal function. This is evidenced by impairments in motor and social behavior, D1-SPN hyperexcitability, and identification of hundreds of differentially regulated genes in D1-SPNs upon loss of both Foxp1 and Foxp2.

Graphical Abstract

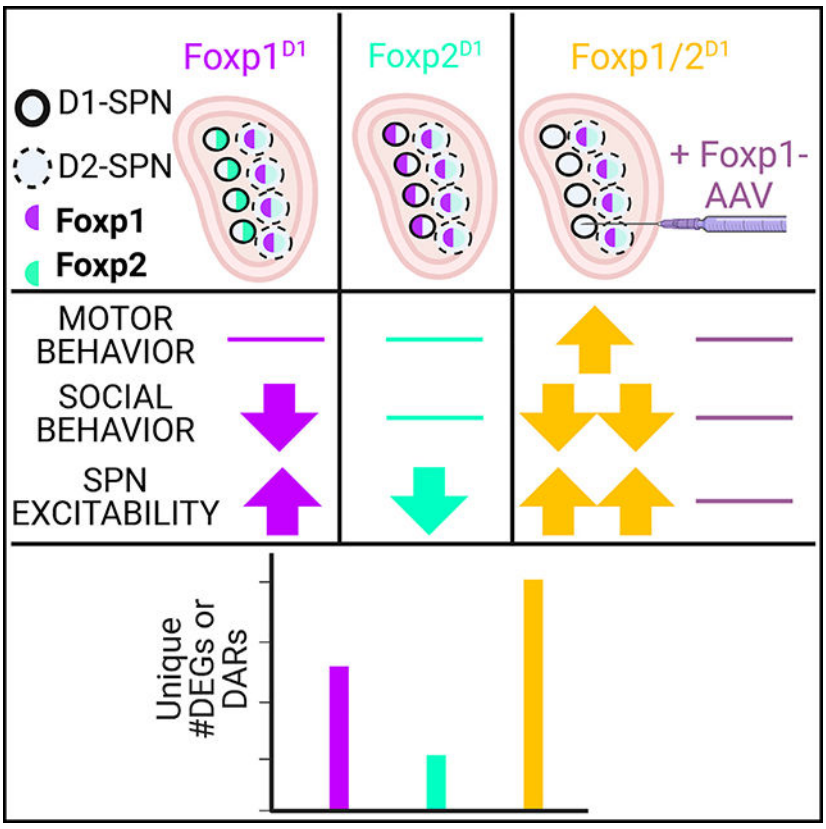

INTRODUCTION

The GABAergic spiny projection neurons (SPNs) of the striatum serve as a hub for important neurochemical messages from different regions of the brain. These inhibitory neurons receive dopaminergic input from the midbrain, particularly the substantia nigra (SN) and ventral tegmental area (VTA), as well as glutamatergic inputs from the thalamus and cortex. The SPNs are the primary cell type in the striatum, the input nucleus of the basal ganglia, and play a key role in the ability of the striatum to coordinate motor activity and reward-based behavior. There are two main classes of SPNs: the dopamine receptor 1 (D1)-expressing SPNs that control the direct pathway, and the dopamine receptor 2 (D2)-expressing SPNs that mediate the indirect pathway.[1–6] Dysregulation of striatal circuits is implicated in many neurodevelopmental disorders (NDDs), such as autism spectrum disorder (ASD), attention-deficit/hyperactivity disorder (ADHD), and Huntington's disease (HD), among others.[4,5,7–12] To understand the molecular mechanisms underlying these and

other diseases of the striatum, it is crucial to study the factors that regulate the proper development and function of the SPNs.

Transcription factors play an essential role in the regulation of gene expression patterns that underlie the specific development, structure, and behavior of individual cell types. Specific transcription factors have been found to play a key role in the differentiation, migration, and survival of striatal neurons.[13] Furthermore, genetic variants in transcription factors have a high risk for disease susceptibility.[14,15] The forkhead box transcription factors (Fox) are a large family of transcription factors that share a common DNA binding domain. Two paralogous members of this family, FOXP1 and FOXP2, have enriched striatal gene expression and mutations in these genes have been implicated in striatal function.[16–22] The members of the Fox family must dimerize to function properly; this may either be in the form of homodimers or heterodimers between FOXP1 and FOXP2.[23–27] It is thought that transcription factor dimerization between paralogs arose to reduce the evolutionary constraint on the DNA-binding motif of a given protein, thereby allowing for greater flexibility in transcriptional regulation.[28–30] Paralogous transcription factors often have nearly identical motifs and, thus, there can be compensatory binding at target genes by one upon loss of the other.[31] This compensation results in functional redundancy between the two transcription factors.[28,31,32] The extent to which this redundancy occurs, however, depends on the specific transcription factors in question as well as tissue- and cell-type-specific roles. Interestingly, previous studies have found that the FOXP proteins can cooperatively function to maintain proper cell function.[33–36] However, a cooperative role for these proteins in the brain has yet to be described.

Foxp1 and *Foxp2* are both expressed in the D1 SPNs, one of the few neuronal cell types with high co-expression of these genes.[16–18,20,22,37] In contrast, D2 SPNs primarily express Foxp1.[18,20] Foxp1 is crucial for the development and function of the SPNs.[18,19,21,38] Foxp2 has also been linked to striatal function.[39–43] Furthermore, genetic variants in either *FOXP1* or *FOXP2* are among the most significant recurrent *de novo* mutations associated with NDDs. Variants in *FOXP1* rank among the top genes implicated in ASD.[37,44–47] Variants in both genes are also associated with ASD-relevant phenotypes and speech and language deficits.[21,22,37,44,48–63] Both genes have also been implicated in ADHD.[46,64–68]

We previously reported that loss of *Foxp1* from the D2-SPNs results in reduced D2 specification, impaired motor learning, hypoactivity, D2-SPN hyperexcitability, and loss of D2-SPN striatal projections.[18,19] Conversely, many of these deficits are not found in the D1-SPNs upon loss of *Foxp1* except for neuronal hyperexcitability and impairments in social behavior.[18,19,21] Given the specific enrichment of *Foxp2* in the D1-SPNs, this raises the possibility that Foxp2 compensates for the loss of Foxp1. In addition, striatal-specific loss of *Foxp2* also showed no major motor learning impairments, indicating reciprocal compensation by *Foxp1*.[69] Previous work in non-neuronal tissue has investigated the synergy between *Foxp1*, *Foxp2*, and the closely related *Foxp4* where studies have found differing levels of cooperativity and redundancy between the transcription factors, depending on the cell type.[33–36] In addition, the cooperative role of *Foxp2* and *Foxp4* in neuroepithelial maturation has been documented.[70] However, reports on the simultaneous loss of *Foxp1* and

Foxp2 from the same brain cell type are lacking. Given the co-expression of the two genes in D1-SPNs, we sought to uncover a role for functional cooperativity.

Using a cell-autonomous strategy to delete *Foxp1*, *Foxp2*, or both from D1-SPNs, we examined behavioral, electrophysiological, and transcriptomic differences in mice. In comparison to double-knockout mice, the single knockouts had less severe alterations in all three categories. Thus, we find evidence of compensation between the two transcription factors to maintain striatal function due to complementary roles between *Foxp1* and *Foxp2*.

RESULTS

Generation of mice with Drd1-specific loss of *Foxp1* and/or *Foxp2*

To investigate Foxp1 and Foxp2 function in D1-SPNs, we generated conditional knockout (cKO) mice of *Foxp1*, *Foxp2*, or both in neurons using Cre driven by the *Drd1* promoter (see STAR Methods). Forkhead protein nomenclature follows established guidelines.[71] We generated the following mice: $Drd1^{cre/+}$; $Foxp1^{flox/flox}$ ($Foxp1^{D1}$, deletion of Foxp1 from the D1-SPNs), $Drd1^{cre/+}$; $Foxp2^{flox/flox}$ ($Foxp2^{D1}$, deletion of Foxp2 from the D1-SPNs), $Drd1^{cre/+}$; $Foxp1^{flox/flox}$; $Foxp2^{flox/flox}$ ($Foxp1/2^{D1}$, deletion of both Foxp1 and Foxp2 from the D1-SPNs) and control (mice with floxed genes but no Cre) (Figure 1A). Since *Drd1*.Cre is expressed starting at embryonic day 14.5 (E14.5),[18] *Foxp1* and *Foxp2* are deleted early in striatal development. Mice were also bred to express *Drd1-tdTomato*.[18,19] Reduction of Foxp1 was previously confirmed in $Foxp1^{D1}$ mice.[18] We again confirmed the reduction of Foxp1 as well as the reduction of Foxp2 in relevant genotypes via immunohistochemistry at postnatal day 56 (P56) (Figures 1B–1E).

Using this genetic strategy, we expected Foxp1 expression to be primarily limited to the D2-SPNs.[18,20] To confirm that any remaining Foxp1 expression is not from D1-SPNs, we quantified Foxp1 expression in D1-SPNs as marked by tdTomato. Compared to controls and $Foxp2^{D1}$ mice, $Foxp1^{D1}$ mice had significantly reduced Foxp1 in the D1-SPNs, as indicated by reduced overlap with tdTomato (Figures S1A–S1G). Likewise, we confirmed D1-SPN-specific reduction of Foxp2 in the striatum of $Foxp2^{D1}$ mice (Figures S1A–S1F and S1H). There is some residual expression of *Foxp1* and *Foxp2* in the D1-SPNs. This is likely because cells express *Foxp1* and/or *Foxp2* before Cre expression.[18]

snRNA-seq of Drd1 SPNs in juvenile mice with loss of *Foxp1* and/or *Foxp2*

We had previously determined the cell-type-specific transcriptional targets of Foxp1 in the juvenile striatum but hypothesized that there may be compensation by Foxp2.[18] Therefore, we carried out single-nucleus RNA sequencing (snRNA-seq) experiments in dorsal striatal tissue with loss of *Foxp1*, *Foxp2*, or both in the mouse brain at P9. We profiled tissue from three mice from each genotype. After quality-control filtering, we compared 190,082 nuclei across all four genotypes (Figures S2A and S2B). We found 11 major cell types represented across clusters, which were distributed largely equally across genotypes (Figures S2C–S2E). SPNs were then subset and re-clustered to determine the contribution of each genotype to major SPN cell types (D1, D2, and eccentric SPNs [eSPNs]; Figures 2A and S2F).[72] These

subsetted clusters were also filtered for quality using the same cutoffs retaining 52,124 D1-SPNs for further analysis (Figures S2A and S2G).

Differentially expressed genes in juvenile D1-SPNs reveal compensation between Foxp1 and Foxp2

We next determined the differentially expressed genes (DEGs) within each cell type. Each cKO condition was compared to controls and genes were considered differentially expressed based on previously used criteria (false discovery rate [FDR] <0.05 and an absolute log fold change [logFC] >0.25).[18] We observed 289 genes changing in the $Foxp1^{D1}$ (126 up, 163 down), 89 in the $Foxp2^{D1}$ (79 up, 10 down), and 213 in the $Foxp1/2^{D1}$ (142 up, 71 down) D1-SPNs (Figures 2A and 2B). There was limited but, in some cases, significant overlap between any of the conditions. There were 21 genes overlapping between $Foxp1^{D1}$ and $Foxp1/2^{D1}$ (Fisher's exact test: 2.08, $p = 0.001$), only five between $Foxp2^{D1}$ and $Foxp1/2^{D1}$ (Fisher's exact test: 1.61, $p = 0.2$), and 22 between $Foxp1^{D1}$ and $Foxp2^{D1}$ (Fisher's exact test: 5.22, $p = 7.49 \times 10^{-11}$). Of the 213 $Foxp1/2^{D1}$ D1-SPN DEGs, 189 (89%) were unique to that condition. These genes should represent those with *Foxp1* and *Foxp2* compensatory regulation as differential expression is only observed upon the loss of both genes. Among these 213 genes, two-thirds are upregulated, in line with previously noted repressive roles of these transcription factors (Figure 2C).[23,26,37,73]

While the overlap of DEGs between the different knockout conditions is limited, certain comparisons indicate shared regulatory mechanisms. Of the 22 genes overlapping between the $Foxp1^{D1}$ and $Foxp2^{D1}$ D1-SPNs, 19 changed in the same direction (Figure 2B; Table S1). These represent genes regulated similarly by both transcription factors when one is lost. Using our logFC cutoffs, there was limited overlap between the single knockouts, but we considered that we may be missing some genes that are changing in the same direction. These genes are important to note, as they represent genes that are similarly up- or downregulated by each transcription factor without compensation by the remaining factor. To determine the extent of such independent regulation, we performed a rank-rank hypergeometric overlap (RRHO) and found significant overlap in the direction of change in gene expression in the overall gene set when comparing single knockouts (Figure S2H). There were only two genes that overlapped among all three conditions, one of which was the cAMP/cGMP associated gene Phosphodiesterase 1B (*Pde1b*). This gene was upregulated in the single knockouts but downregulated in the double cKO (Table S1), pointing toward a pattern of compensation. We overlapped the juvenile DEGs with a list of high-confidence genes related to ASD and found enrichment with DEGs from all three cKOs (Figure 2D; Table S1). We also carried out Gene Ontology (GO) analysis of the DEGs and identified enrichment of similar functional terms for each knockout (in particular, categories associated with electrophysiological properties including synaptic function; Figures 2E–2G; Table S1). Our snRNA-seq in juvenile mouse D1-SPNs reveals hundreds of genes that are regulated by both *Foxp1* and *Foxp2*. These are genes that are only differentially regulated upon the loss of both transcription factors, consistent with a pattern of compensation between the two transcription factors.

To confirm some of our snRNA-seq findings, we used single-molecule fluorescent *in situ* hybridization (smFISH) to verify the change in gene expression in exemplary genes in our single knockouts. We probed for *Ntn1* (downregulated in Foxp1^{D1} D1-SPNs) and *Cdk7* (downregulated in Foxp1^{D1} and Foxp2^{D1} D1-SPNs) and analyzed their expression in the D1-SPNs. We probed for expression of these genes in D1-SPNs (marked by the gene Tac1). We found that *Ntn1* was indeed downregulated in the Foxp1^{D1} D1-SPNs but not in D1-SPNs of Foxp2^{D1} mice, as expected (Figures 3A–3C). *Cdk7* was also downregulated in Foxp1^{D1} D1-SPNs and showed a trend toward downregulation in Foxp2^{D1} D1-SPNs, although this does not quite reach significance (Figures 3D–3F).

Identification of differentially accessible chromatin regions in D1 SPNs with loss of *Foxp1* and/or *Foxp2*

To determine regulatory mechanisms underlying differential gene expression with loss of *Foxp1* and/or *Foxp2*, we carried out single-nucleus assay for transposase-accessible chromatin with sequencing (snATAC-seq) experiments in P9 mice. After quality-control filtering, we profiled 75,935 nuclei from 12 mice (three mice/genotype; Figure S3A). We annotated 36 clusters using label transfer from the juvenile snRNA data (Figure 4A). All genotypes were represented across the different cell types (Figure S3B). We determined that the number of peaks, percentage of reads in peaks, and number of reads in peaks were largely similar across genotypes (Figures S3C–S3E). We next determined the differential accessibility regions (DARs) for each knockout condition in comparison to controls in the D1-SPN clusters. Interestingly, there were far more DARs in the Foxp1/2^{D1} D1-SPNs than in any other condition. We identified 237 genes with DARs in the Foxp1^{D1}, 410 in the Foxp2^{D1}, and 1,732 in the Foxp1/2^{D1} condition (Figure 4B; Table S2). There was more overlap between the DARs of each condition than we found for DEGs from this same time point. We found 39 DARs shared between the single-knockout conditions (Fisher's exact test: 10.74, $p = 1.78 \times 10^{-58}$), 51 between the Foxp1^{D1} and Foxp1/2^{D1} (Fisher's exact test: 2.65, $p = 3.07 \times 10^{-16}$), 149 between Foxp2^{D1} and Foxp1/2^{D1} (Fisher's exact test: 3.15, p $= 2.82 \times 10^{-43}$), and 46 DARs shared among all three conditions (Fisher's exact test: 3.53, $p = 3.1 \times 10^{-38}$; Figure 4B). Similar percentages of DARs were unique for single cKOs (101/237, 43%, Foxp1^{D1}; 177/410, 43%, Foxp2^{D1}); however, most DARs in the double cKO are unique (1,486/1,732; 86%). This indicates that there is compensation occurring in each single cKO as the loss of both transcription factors resulted in the observation of much greater alteration in chromatin accessibility. We next asked whether genes associated with DARs overlapped with DEGs in the double-cKO mice. Among the 213 DEGs in Foxp1/2^{D1} D1-SPNs, 45 (21%) also had a DAR associated with the same gene (Figure 4C).

Foxp1 and *Foxp2* genes are classically thought to be repressors.[23,26,37,73] However, changes in chromatin accessibility were roughly equivalent for more open (739) and more closed (853) DARs in the double cKOs. In contrast, single-cKO lines had mostly open DARs with 209 open and 19 closed DARs in Foxp1^{D1} and 303 open and 69 closed DARs in Foxp2^{D1} (Figure 4D). The results in the single-cKO mice support a repressive role for these transcription factors but, upon the loss of both factors, there are likely indirect mechanisms also at play. Consistent with our snRNA-seq findings, we again report that loss of both

Foxp1 and *Foxp2* results in large-scale dysregulation of the chromatin regions in the D1-SPNs.

FOXP motif enrichment among DARs

We next investigated whether the regions regulated by the Foxp transcription factors were direct targets or the result of further downstream regulation. Methods to determine transcription factor binding to DNA at genome-wide scale are challenging to carry out in a cell-type-specific manner. Therefore, we harnessed the snATAC-seq data to determine potential direct versus indirect targets of Foxp1 and Foxp2 in D1-SPNs by assessing transcription factor motif enrichment in DARs from each cKO. Using cutoffs of FDR < 0.05 and a fold enrichment of at least 1.75 within each DAR, we found enriched motifs within D1-SPNs. Foxp1^{D1} DARs had the fewest enriched motifs with only 18. Foxp2^{D1} DARs had 64 enriched motifs, whereas Foxp1/2^{D1} DARs were enriched for 446 transcription factor-binding motifs. Again, we found that results from Foxp1/2^{D1} cells were the most different, with these DARs containing the greatest number of unique motifs (342/446; 77%), whereas the single cKO had fewer motifs unique to a specific genotype (only 1/18 for Foxp1^{D1} and 16/64 for the Foxp2^{D1}; Figure 4E). The motifs from the single knockouts were significantly overlapping with each other (Fisher's exact test: 8.42; $p = 2.51 \times 10^{-11}$) and with the double knockouts (Foxp1^{D1} overlap with Foxp1/2^{D1}, Fisher's exact test, 1.79, $p = 0.001$; Foxp2^{D1} overlap with Foxp1/2^{D1}, Fisher's exact test, 1.42, $p = 0.001$). Interestingly, in the single knockouts, all enriched motifs were in DARs that were more accessible, whereas, in the double cKOs, the motifs were enriched in both more accessible regions (118 motifs) as well as more closed DARs (224; Figure 4F). This is consistent with the patterns observed in the DARs where the single cKOs primarily had differentially open chromatin, whereas the double cKO had greater dysregulation resulting in both more open and more closed chromatin.

Given the presumed repressive role of Foxp1 and Foxp2, we hypothesized that there would be Fox motifs in the DARs associated with more open regions. This was indeed the case in the Foxp1/2^{D1} as 29/118 (25%) of the enriched motifs in more accessible chromatin regions were Fox motifs, including motifs for Foxp1 and Foxp2 (Figure 4F; Table S2). There were no such motifs enriched in more closed chromatin regions. We also identified 693 genes that contained a Fox motif enriched within an associated DAR in the double cKO (Table S2). This suggests that 693/739 (94%) genes with more open DARs are potentially directly regulated by both Foxp1 and Foxp2. Examples of such genes include Phosphodiesterase 1C (*Pde1c*), which, like *Pde1b*, is involved in cAMP regulation, and *Kcnip1*, the potassium voltage-gated channel interacting protein 1 (Figures 4G and S3F).

To investigate this further, we identified the predicted targets of Foxp1 and Foxp2 among these 693 DARs. There were 165 predicted targets of Foxp1 and 214 predicted targets of Foxp2. Of these, 117 of these DARs have motifs enriched for both Foxp1 and Foxp2 (Table S2). Interestingly, this leaves 431 DARs with enriched motifs for other Fox proteins. *Foxp4*, which is expressed during development but to a considerably lesser extent in postnatal striatum, was not among the Fox proteins with enriched motifs.[37,74] Motifs for Foxo1, which is one of the few non-Foxp genes expressed in the SPNs, was found to be enriched in

241 of these DARs, 112 of which were non-overlapping with predicted targets of Foxp1 and/or Foxp2 (Table S2).[75,76] This gene was also recently determined to be a downstream target of Foxp1 and is also downregulated in the Foxp1/2^{D1} D1-SPNs (adjusted p value = 2.98×10^{-30}).[77] Given that these DARs are only present in the Foxp1/2^{D1} D1-SPNs, this implies downstream effects of the loss of *Foxp1* when *Foxp2* is also absent and unable to compensate. This still leaves 319 enriched Fox motifs not explained by loss of *Foxp1* or *Foxp2*. Given the similarities between motifs of all Fox proteins, these could be targets of Foxp1 and/or Foxp2 that our analysis was not able to disambiguate or could represent other methods of regulation. Further work will need to be done to determine the precise mechanisms of DAR regulation. The lack of Fox motif enrichment in genes associated with more closed DARs implies that, while loss of both genes can result in closed chromatin, the dysregulation is likely mediated through indirect mechanisms. To further support the idea that compensation is occurring, there were no enriched Fox motifs in either single-knockout condition in both open and closed DARs.

Among non-Fox motifs that were enriched in DARs and potentially of interest for understanding striatal function, we noted motifs for the Myocyte Enhancer Binding Factor-2 (Mef2) family of transcription factors in both open and closed DARs in the Foxp1/2^{D1} data. Members of this family of transcription factors are known to be directly repressed by Foxp1 or Foxp2.[39,78] Some of the genes indirectly dysregulated could thus be attributed to dysregulation of *Mef2* genes due to loss of *Foxp1* and *Foxp2*. In sum, we report that loss of both Foxp1 and Foxp2 results in a greater amount of altered chromatin state in comparison to either single-knockout condition, indicating robustness between the two genes. These DARs are associated with motifs enriched for binding by forkhead box proteins and their known targets.

Foxp1 and *Foxp2* synergistically mediate D1-SPN hyperexcitability

We previously reported that either a full-body heterozygous deletion or a D2-SPN-specific loss of *Foxp1* results in increased intrinsic excitability of the D2-SPNs.[19,21] These changes are at least partially driven by the downregulation of channels regulating potassium inward rectifying (K_{IR}) currents such as the potassium voltage-gated channel subfamily J members 2 (*Kcnj2*) and 4 (*Kcnj4*) and potassium leak (K_{Leak}) currents such as the potassium two-pore-domain channel subfamily K member 2 (*Kcnk2*).[18,19] We also observed increased excitability in the D1-SPNs in the Foxp1^{D1} mice, albeit to a lesser degree.[19] This attenuated phenotype suggested the possibility that loss of Foxp1 might be partially compensated for by *Foxp2*. To investigate this, we performed current-clamp experiments in juvenile mice (P14-P18). Expression of *Drd1-tdTomato* was used to identify D1-SPNs in slices. Foxp1^{D1} D1-SPNs had increased excitability compared to controls as observed by plotting the number of action potentials as a function of injected current amplitude (Figure 5A). D1-SPNS in Foxp1/2^{D1} mice were more hyperexcitable, even in comparison to the Foxp1^{D1} mice, including at lesser current injections (Figures 4A and S4A). Changes in subthreshold membrane properties likely contribute to the observed hyperexcitability as both Foxp1^{D1} and Foxp1/2^{D1} D1-SPNs show increased input resistance (Figure 5B). Conversely, Foxp2^{D1} D1-SPNs show significant hypoexcitability compared to controls (Figure 5A). Based on our previous work, we hypothesized that this hypoexcitability could be due to increased

expression of *Foxp1*.[18] Indeed, when we used fluorescence-activated cell sorting (FACS) to sort for tdTomato positive D1-SPNs from Foxp2^{D1} mice at P14, we found increased *Foxp1* expression compared to controls via RT-qPCR (Figure S4B). Thus, while we now find that *Foxp2* also plays a role in the regulation of intrinsic excitability of SPNs, the role of *Foxp1* appears to eclipse that of *Foxp2*.

Changes in knockout mice are driven by impaired K_{Leak} channel function

We previously reported that the hyperexcitability of D2-SPNs with loss of *Foxp1* was due to altered K_{IR} and K_{Leak} currents.[19] To test the role of *Foxp1* in regulation of these currents in the D1-SPNs, we performed a separate set of experiments, this time in the presence of tetrodotoxin (TTX) to block action potentials. For all four genotypes, we utilized a multi-step voltage protocol and measured induced currents. This was done first in control artificial cerebrospinal fluid (ACSF) and then with subsequent wash-in of Cs^+ to block K_{IR} currents.[79] Average current density versus voltage plots (IV plots) were generated for both conditions (Figures S4C and 4D). In the absence of Cs^+, at both depolarized and hyperpolarized potentials, Foxp1^{D1} and Foxp1/2^{D1} D1-SPNs have a current density lower than that of the controls or Foxp2^{D1} mice (Figure S4C). These differences are still detected when Cs^+ is applied to the bath (Figure S4D). Consistent with these results, D1-SPNs in Foxp1^{D1} and Foxp1/2^{D1} mice show increased input resistance in Cs^+ wash-in conditions (Figure S4E). We subtracted traces collected in the presence of Cs^+ (Figure S4D) from those collected before Cs^+ wash-in (Figure S4C) to obtain currents that are blocked by Cs^+ (Figure 5C). We report that there are no detectable differences between controls and any of the cKOs (Figure 5C). This strongly suggests that K_{IR} channels are unchanged upon the loss of *Foxp1* or *Foxp2* and therefore dysregulation of these channels is not driving the difference seen between genotypes.

In the presence of Cs^+, differences in the IV plots for both Foxp1^{D1} and Foxp1/2^{D1} D1-SPNs persist (in comparison to controls) at hyperpolarized and depolarized potentials. This suggests that a voltage-insensitive current accounts for these differences. Consistent with these results, increased input resistance was observed in the D1-SPNs of these knockouts under Cs^+ conditions (Figure S4E). We speculate that a loss of voltage independent K_{Leak} currents may account for these results, similar to what we found upon loss of *Foxp1* from D2-SPNs.[19] Accordingly, regions associated with *Kcnk2* in the Foxp1/2^{D1} D1-SPNs were in a more repressive chromatin state and dual loss of *Foxp1* and *Foxp2* from the juvenile D1-SPNs results in downregulation of this gene (adjusted p value = 7.7×10^{-86}). Since loss of Kcnk2 is a factor in driving the hyperexcitability phenotype, we hypothesized that increased expression of this gene might underlie hypoexcitability of the D1-SPNs in Foxp2^{D1}. Indeed, we observed increased *Kcnk2* in the D1-SPNs of Foxp2^{D1} in comparison to controls by both RT-qPCR (Figure S4F) and in the snRNA-seq data (adjusted p value = 1.63×10^{-40}), suggesting that *Kcnk2* has compensatory positive regulation by Foxp1 with loss of Foxp2 in D1-SPNs. Together, our data implicate K_{Leak} impairment downstream of loss of Foxp1 and/or Foxp2 in D1-SPNs.

Foxp1 is sufficient to restore D1-SPN excitability to baseline

Our findings indicate a key role for Foxp1 in maintenance of D1-SPN excitability. Loss of *Foxp1* resulted in hyperexcitability, while upregulation of *Foxp1* in the Foxp2^{D1} D1-SPNs likely contributed to hypoexcitability. With this in mind, we considered that *Foxp1* alone may be sufficient to maintain neuronal excitability even in the D1-SPNs of double knockouts. To test this, we used an adeno-associated virus (AAV) construct to reintroduce Foxp1, under the neuronal *Syn1* promoter. This construct also results in expression of GFP for visualization purposes (pAAV-hSYN-Foxp1-T2A-eGFP). Pups were injected at P1 with this construct or a control vector also expressing GFP (AAV9-hSyn-eGFP) into the striatum (Figure 5D). As before, current-clamp experiments were performed on juvenile mice between P14 and P18, this time with recordings done on cells that expressed both tdTomato and GFP. In mice with the Foxp1 construct, we no longer saw neuronal hyperexcitability of the D1-SPNs (Figure 5E). Likewise, the input resistance returned to baseline (Figure 5F). Thus, re-introduction of *Foxp1* at an early postnatal time point in Foxp1/2^{D1} mice is sufficient to rescue the hyperexcitability phenotype seen in these mice.

In summary, these results show that loss of *Foxp1* from the D1-SPNs results in hyperexcitability. The further loss of *Foxp2* from these neurons amplifies this result. We speculate that hyperexcitability may arise from loss of K_{Leak} channels. Conversely, there is neuronal hypoexcitability observed in the Foxp2^{D1} mice, seemingly driven by an increase in *Foxp1*. While both *Foxp1* and *Foxp2* play roles in maintaining D1-SPN excitability, *Foxp1* has a greater role, as shown by its sufficiency to rescue hyperexcitability phenotypes in Foxp1/2^{D1} mice.

Persistent cell-type genomic changes in the striatum with loss of *Foxp1* and/or *Foxp2*

We next asked whether developmental loss of Foxp1 and/or Foxp2 results in sustained gene expression changes in D1-SPNs. Thus, we carried out snRNA-seq in dorsal striatal tissue from mice at P56. Using the same quality-control filtering as before, we profiled 202,611 nuclei across all four genotypes with three mice per genotype (Figures S5A and S5B). We identified 11 major cell types that were represented equally across genotypes (Figures S5C–S5E). To determine D1-SPN relevant changes, SPNs were subset and re-clustered for further analysis (Figure 6A). A total of 14,465 D1-SPNs were maintained, and representation of each genotype remained roughly equal (Figures S5A and S5F). These subset clusters were also filtered for quality using the same standards (Figure S5G).

We again determined DEGs in each cell type using the same criteria. In the D1-SPNs, we found 222 genes changing in the Foxp1^{D1} (108 up, 114 down), 240 in the Foxp2^{D1} (188 up, 52 down), and 520 in Foxp1/2^{D1} (319 up, 201 down; Figures 6B and 6C). There were 362 genes unique to the double-knockout condition (70% of all Foxp1/2^{D1} D1-SPN DEGs). We hypothesize that these are genes that are normally compensated by either *Foxp1* or *Foxp2*. Over 60% of these genes are differentially upregulated upon the loss of both transcription factors, implicating a primarily repressive role under normal conditions.

There was greater overlap of DEGs between conditions than was seen in juveniles, and these overlaps were somewhat limited yet significant. There were 76 genes overlapping between

Foxp1^{D1} and Foxp1/2^{D1} (Fisher's exact test: 4.02, $p = 1.93 \times 10^{-28}$), 103 between Foxp2^{D1} and Foxp1/2^{D1} (Fisher's exact test: 5.04, $p = 1.38 \times 10^{-44}$), and 29 between Foxp1^{D1} and Foxp2^{D1} (Fisher's exact test: 3.32, $p = 7.65 \times 10^{-9}$). Among the 29 shared genes between Foxp1^{D1} and Foxp2^{D1}, 23 were changed in the same direction, indicating similar types of regulation. There were 21 genes changing in the same direction among all three conditions (Figure 6B; Table S1). We again performed RRHO between the single-knockout conditions to determine how gene expression changes in the absence of a logFC cutoff. We again found that genes were similarly up- or downregulated in Foxp1^{D1} and Foxp2^{D1} D1-SPNs (Figure S5H). We overlapped all DEGs with ASD-relevant gene lists and once again found enrichment for ASD-risk genes (Figure 6D; Table S1). GO analysis of the DEGs for all three conditions resulted in similar terms to what we observed in the juveniles (Figures 6E–6G; Table S1). This indicates that, although few specific DEGs are shared between the two time points, the loss of *Foxp1* and/or *Foxp2* affects similar gene pathways in the adult and juvenile striatum. Findings in adult snRNA-seq match the trends observed in the juvenile D1-SPNs, supporting evidence of sustained functional compensation between *Foxp1* and *Foxp2* throughout the lifespan.

We also collected and annotated cortical cells in the adult dataset. Since *Foxp1, Foxp2*, and *Drd1* are all expressed in the cortex, we could examine whether D1-Cre affects *Foxp1* and/or *Foxp2* transcriptional programs in D1-positive cortical cells.[80] We identified DEGs in 10 cortical cell types that express *Drd1*. Of the 30 (three genotypes, 10 cell types for each) comparisons that we made, 22 had fewer than 20 DEGs and only excitatory intra-telencephalic layer 6 neurons in the Foxp1^{D1} mice exhibited more than 50 DEGs (Figure S5I; Table S1). This indicates limited transcriptional changes in the cortex compared to the striatum upon the loss of *Foxp1* and/or *Foxp2* using a D1-Cre. ASD-risk genes were observed among the cortical DEGs in specific cell types, but more work is needed to determine how dysregulation of these genes in the cortex might affect the results presented here (Table S1).

Loss of both *Foxp1* and *Foxp2* results in impaired motor and social behavior in mice

We next determined the consequences of the transcriptional changes in the adult mice by assessing behavior in 8- to 12-week-old mice. Previous studies identified motor-learning, activity, and social-behavior impairments in mice with loss of either *Foxp1* or *Foxp2*.[18,21,37,53,69,81–86] We assessed motor learning via the accelerated rotarod. While individual deletion of one gene did not result in significant changes, the Foxp1/2^{D1} mice showed a significant impairment compared to controls (Figure 7A). There were no differences in grip strength between any of the genotypes (Figures S6A and S6B). These findings are consistent with the hypothesis that *Foxp1* and *Foxp2* can functionally compensate for each other to regulate motor activity. Findings with deletion of only *Foxp1* also match our previous findings.[18]

To assess social behavior in adult mice, we tested nest building, a communal behavior that can be reproducibly quantified in rodents.[18,87] While the Foxp2^{D1} mice have no deficit in nest building, Foxp1^{D1} mice created significantly fewer well-developed nests, in line with our previous findings.[18] The Foxp1/2^{D1} mice, however, demonstrated even significantly

greater nest-building impairments (Figure 7B). This indicates that *Foxp2* is not sufficient to fully rescue the effects of *Foxp1* deletion in this social behavior. Instead, the loss of *Foxp2* in addition to *Foxp1* further exacerbates the nest-building deficits. We also examined pup isolation ultrasonic vocalizations (USVs), which are calls made by mouse pups to elicit maternal care. While we previously reported that Foxp1^{D1} mice made fewer calls than controls,[18] we were unable to replicate this finding in the same genotype in this study. Furthermore, neither the Foxp2^{D1} nor the Foxp1/2^{D1} mice showed any deficiencies in the number of USV calls (Figure S6C). These findings indicate that *Foxp1* and *Foxp2* have mostly redundant functional roles in regulating motor and social behaviors in adult mice. However, *Foxp1* has a greater impact compared to *Foxp2*, as indicated by the nest-building impairment observed in Foxp1^{D1} mice.

Viral-mediated re-expression of *Foxp1* is sufficient to restore behavioral impairments

We next asked whether expression of *Foxp1* is sufficient to restore behavioral deficits in Foxp1/2^{D1} mice, similar to its restorative effects on neuronal excitability. We injected either a control or Foxp1-expressing construct bilaterally into the striatum of P1 pups and assessed behavior at 8–12 weeks. The double knockouts with restored Foxp1 no longer show an impairment in rotarod (Figure 7C) or nest building (Figure 7D). Thus, re-introduction of *Foxp1* at an early postnatal time point was sufficient to restore behavioral impairments observed in adult Foxp1/2^{D1} mice.

DISCUSSION

Here, we examined overlapping and unique functions of the transcription factors Foxp1 and Foxp2 in striatal D1-SPNs. Using conditional mouse models to specifically knock out *Foxp1*, *Foxp2*, or both from the D1-SPNs, we found that the combined loss of both genes amplified impairments in K_{Leak}-mediated hyperexcitability as well as motor and social behaviors, indicating compensatory roles of these two transcription factors. Our data show that forkhead motifs are enriched in regions of chromatin that are more accessible in D1-SPNs in double-cKO mice. We propose two primary mechanisms of compensation. In the first scenario, either *Foxp1* or *Foxp2* can regulate a given gene. The loss of one transcription factor results in maintained regulation by the other, and only upon loss of both factors is gene expression altered (represented by DEGs unique to Foxp1/2^{D1}). In the second scenario, loss of one transcription factor leads to increased regulation of the target gene by the remaining gene but decreased regulation upon loss of both (represented by DEGs overlapping in the same direction between single cKOs and moving in the other direction in the double knockouts). Based on the limited overlap of transcriptional targets between the single knockouts, we suggest the first mechanism as the primary method through which compensation occurs (Figure S7).

Our data indicate that there may be other forms of compensation that are occurring. While one primary method is shown in Figure S7, there are other possibilities to consider. Some DEGs are trending in the same direction but are not represented in Figures 2 and 6 due to the stringency of cutoffs. However, as indicated by the RRHO, there is a correlation between the gene expression observed in the single-knockout conditions. Thus, there may

be genes that are in fact targets of both Foxp1 and Foxp2 but are preferentially targeted by one over the other. An example already mentioned is *Kcnk2* (Figure S8A), a gene that is seemingly a target of both Foxp1 and Foxp2 as loss of both transcription factors amplifies *Kcnk2*-mediated electrophysiological impairments. However, loss of *Foxp1* is sufficient to drive some electrophysiological impairments, indicating that Foxp2 is not a sufficient regulator of this gene. Interestingly, there seems to be over-regulation of expression of *Kcnk2* upon loss of *Foxp2*, indicating that a balance of Foxp1 and Foxp2 expression is needed to properly regulate this gene. There may also be genes that are only a target (direct or indirect) of one transcription factor but can become regulated by the other transcription factor upon the loss of its normal regulator. These may be represented in DEGs unique to the double knockouts. For example, a gene might be a target of Foxp2. However, upon loss of Foxp2, Foxp1 assumes this gene as a target, thereby maintaining regulation (Figure S8B). Another possibility would be genes that are regulated by both transcription factors. However, loss of one transcription factor results in overactivation of this gene, perhaps to maintain molecular function that would otherwise be dysregulated. For example, *Pde1b* has increased expression upon loss of either *Foxp1* or *Foxp2*. This gene, involved in regulation of cGMP hydrolysis, may be upregulated to maintain cGMP hydrolysis, which may otherwise be disrupted due to dysregulation of other genes in this pathway.[88] These other genes may (like *Pde1b*) be represented by genes overlapping between all three conditions (Figure S8C). However, some genes may only overlap between the single knockouts. Given the lack of overlap between single-knockout DEGs, such genes could be trending in the same direction without reaching the stringency cutoffs. Thus, there are many additional possible mechanisms of gene regulation to interpret our results and any of these would require further work to validate.

While our results provide evidence of functional compensation, we acknowledge that other forms of compensation may not be addressed by our experimental approaches, such as those that include additional genes or gene regulatory mechanisms. For example, target genes may be preferentially bound by a heterodimer of Foxp1 and Foxp2, but regulation is maintained by a homodimer of the remaining factor upon loss of one. The similarity in DNA binding motifs of the two transcription factors makes it challenging to definitively distinguish between these possibilities. Compensation may also occur through coregulation of transcription factors downstream of Foxp1 and Foxp2. For example, it is only in the Foxp1/2^{D1} D1-SPNs that we observed enriched Mef2 motifs within DARs. The Mef2 family of genes, which are known to be downregulated by *Foxp1* and *Foxp2*,[21,31,39,54,78] may thus be regulated in a compensatory manner. Upon loss of both Foxp genes, we propose that there is dysregulation of not only Foxp1/Foxp2 targets but also Mef2 family transcriptional targets. *Mef2a*, *Mef2c*, and *Mef2d* are all upregulated in juvenile (adjusted p value = 4.23×10^{-54}, 5.04×10^{-32}, and 1.81×10^{-29}, respectively) while only Mef2c was upregulated in the adult (adjusted p value = 0.0008) Foxp1/2^{D1} D1-SPNs, adding further evidence to this possibility.

While we observed genome-wide molecular compensation occurring in the double-cKO data, we also identified genes that are uniquely regulated by either Foxp1 or Foxp2, indicating some lack of robustness between the two transcription factors (although the RRHO data suggest cutoff decisions affect these overlaps). The non-overlapping DEGs

in the single knockouts represent genes that are strongly regulated by either *Foxp1* or *Foxp2*. This indicates that, despite their similarities, there are distinct targets for each transcription factor. Functional evidence to support these molecular findings is observed in the Foxp1^{D1} mice that have electrophysiological and behavioral phenotypes not seen in controls, indicating that *Foxp2* is not fully compensating for loss of *Foxp1*.

D1-SPNs in Foxp1^{D1} mice have K_{Leak}-mediated increases in neuronal excitability, which is amplified in the Foxp1/2^{D1} mice. Thus, while loss of Foxp1 is sufficient to develop a phenotype, *Foxp2* still plays a role as shown by the exacerbated hyperexcitability. The hypoexcitability observed in Foxp2^{D1} D1-SPNs represents a scenario wherein *Foxp1* "overcompensates" and increases regulation of genes involved in mediating neuronal excitability. In support of this idea, we found that *Kcnk2*, a gene we identified as mediating hyperexcitability in D2-SPNs,[19] was specifically upregulated in the Foxp2^{D1} D1-SPNs. Furthermore, AAV-mediated overexpression of Foxp1 is sufficient to restore neuronal excitability in Foxp1/2^{D1} mice, indicating that *Foxp1* is sufficient to compensate for loss of *Foxp2*. Our study focused on the potential contribution of K_{IR} and K_{Leak} channels to neuronal hyperexcitability. However, other types of potassium channels show differential expression upon loss of both *Foxp1* and *Foxp2*, including the potassium voltage-gated channels *Kcnip1* and *Kcnb1*. Interestingly, variants in the latter have been implicated in apraxia of speech, a phenotype seen in human patients with mutations in Foxp1 or Foxp2.[60,61,89] Future studies can determine how the downregulation of these genes may affect the phenotypes we observe.

We report that motor learning was only impaired upon loss of both genes, indicating that *Foxp1* and *Foxp2* can robustly compensate to maintain circuits dictating motor behavior. Reexpression of Foxp1 was sufficient to restore motor learning to baseline levels in the Foxp1/2^{D1} mice. Thus, each gene can maintain proper SPN function for overall movement with impairments only arising when both genes are deleted. Unlike motor behavior, social behavior (as measured by nest building) is impaired upon the loss of *Foxp1* alone, highlighting a requirement for *Foxp1* in that circuit. However, the impairment is exacerbated upon further loss of *Foxp2*, indicating that *Foxp2* synergizes with *Foxp1* function in this behavior. We note that FoxP2 expression can change during neuronal activity in songbirds and is predicted to be downregulated by neuronal activity in mammals as well.[90–92] Thus, future studies that examine the impact of Foxp2 and Foxp1 transcriptional function in D1-SPNs immediately following behavioral manipulations could be informative.

We identified hundreds of genes regulated by both *Foxp1* and *Foxp2*. Given the important role of these transcription factors in human brain disorders, the contribution of these DEGs to disease-relevant D1-SPN development and function should be assessed. For example, members of the neurexin family of genes (*Nrxn1*, *Nrxn2*, and *Nrxn3*), which have been implicated in ASD, were differentially regulated.[93,94] Recent studies report that loss of *Nrxn1* impaired synaptic connections onto the SPNs,[95,96] but the roles of neurexins in D1-SPN development are yet to be studied. We also identified many genes crucial for regulating the G-protein signaling cascade, which is required for proper D1-SPN function, such as *Pde1b*, *Pde1c*, protein kinase C alpha (*Prkca*), and protein kinase C beta (*Prkcb*).[97–104] Adenylyl cyclase 5 (*Adcy5*), which also mediates G protein-coupled receptor (GPCR)

signaling and can affect rotarod performance,[105] is downregulated in adult Foxp1/2^{D1} mice. Another recent study identified upregulation of *Dyanactin1* (*Dctn1*), which encodes a subunit of dynein that is important for regulation of motor homeostasis in striatal neurons, in mice with *Foxp2* mutations.[106] In juvenile Foxp1/2^{D1} D1-SPNs, *Dctn1* had a more permissive chromatin state and was upregulated (adjusted p value = 1.12×10^{-12}). Thus, alterations in these genes result in striatal dysfunction and provide compelling avenues for follow-up studies downstream of Foxp1 and Foxp2 in the striatum.

In summary, we find that Foxp1 and Foxp2 have compensatory roles in the D1-SPNs. Here, we investigate the interaction between these transcription factors in a neuronal population that expresses both genes. D1-SPNs are crucial for motor behaviors, and it is only upon the loss of both genes that mice showed impairments in motor learning and motor activity. While nest building was impaired upon the loss of *Foxp1*, the impairment was amplified upon the further loss of *Foxp2*, indicating compensation. The same trend was observed in K_{Leak}-mediated D1-SPN hyperexcitability. Reintroducing Foxp1 alone was sufficient to restore behavioral and electrophysiological phenotypes to baseline in Foxp1/2^{D1} mice, indicating that *Foxp1* can compensate for the loss of *Foxp2*. Data from single-nucleus transcriptomics supports the compensatory interactions of both genes as shown by hundreds of DEGs and DARs in the D1-SPNs upon the loss of both genes. Overall, the results presented here provide insight into how the paralogous transcription factors Foxp1 and Foxp2 can work together to mediate D1-SPN development and function.

Limitations of the study

There was a lack of direct binding targets (relevant to Figure 4). While we present snATAC-seq data to address how chromatin accessibility is disrupted by loss of *Foxp1*, *Foxp2*, or both, we are unable to determine how direct binding is affected. Given that these genes are transcription factors, we acknowledge that it would be beneficial to identify whether there is compensation at direct binding sites. However, attempts at *in vivo* chromatin immunoprecipitation sequencing (ChIP-seq) experiments using available antibodies have not been successful. Newer techniques, such as cleavage under targets and release using nuclease (CUT&RUN) and cleavage under targets and tagmentation (CUT&Tag) offer alternative methods that have not yet been performed successfully using available antibodies and techniques. Irrespective of antibody efficacy, inherent limitations persist, as these techniques are typically carried out in bulk tissue. The expression of *Foxp1* in D2-SPNs would thus be confounding, as D2-specific direct binding sites would be present in the data as well. However, recent publications indicate that single-nucleus CUT&Tag may be possible and future opportunities to identify direct binding targets in each mouse genotypes in a cell-type-specific manner may be feasible.[107] Currently, such an approach is technically inaccessible to us, and this remains a limitation of our study.

Effects of Foxp1 overexpression in controls are another limitation (relevant to Figure 5). Our study shows that exogenous expression of Foxp1 in the Foxp1/2^{D1}D1-SPNs results in restoration of neuronal excitability to baseline. Notably, there are trends toward a hypoexcitability phenotype when *Foxp1* expression is increased in Foxp2^{D1} D1-SPNs. These observations might suggest that increased Foxp1 expression in D1-SPNs induces

hypoexcitability. However, such an interpretation of the data is confounded by the result that overexpression of Foxp1 in control cells does not produce the same effect. Thus, a Foxp1 gain-of-function scenario occurs only in the absence of Foxp2. However, in the controls, the persistent expression of Foxp2 occludes Foxp1 from driving a similar response. Although we did not measure Foxp1 expression in individual recorded cells, we acknowledge that there may be variability in the extent of AAV expression in a given cell, potentially influencing electrophysiology rescue experiments. Therefore, the precise impact of Foxp1 overexpression on D1-SPNs remains an open question that necessitates further investigation.

STAR★METHODS

RESOURCE AVAILABILITY

Lead contact—Further information and requests should be directed to and will be fulfilled by the lead contact, Genevieve Konopka (Genevieve. Konopka@utsouthwestern.edu).

Materials availability—Animals and materials generated from this study are available from the lead contact with a completed Materials Transfer Agreement.

Data and code availability

- The sequencing data reported in this paper can be accessed at NCBI GEO with accession number GSE228826. All other acquired data are available upon request to the lead contact.
- Code that was used to perform data pre-processing, clustering, differential gene expression analysis, and differential accessibility region analysis is available at GitHub repository (https://github.com/konopkalab/foxp-striatal-compensation) (https://doi.org/10.5281/zenodo.11094304).
- Any additional information required to reanalyze the data reported in this paper is available from the lead contact upon request.

EXPERIMENTAL MODEL AND SUBJECT DETAILS

Mice—Experiments were performed in accordance with procedures approved by UT Southwestern's Institutional Animal Care and Use Committee (IACUCC #2016–101825). All mice were C57Bl/6J. *Foxp1*$^{flox/flox}$ were originally provided by Dr. Haley Tucker and backcrossed to C57BL/6J to obtain congenic animals.[18,81], *Drd1a-Cre* (262Gsat) were obtained from the Mutant Mouse Resource and Research Center., *Drd1-tdTomato* mice were initially obtained from Dr. Craig Powell.[18] *Foxp2*$^{flox/flox}$ mice were obtained from Jackson Laboratories (Strain# 026259).[123] *Foxp1* $^{flox/flox}$ and *Foxp2* $^{flox/flox}$ mice bred to the Cre and reporter lines were maintained separately for the generation of single-knockout mice while a separate line was used to generate mice that were homozygous for both *Foxp1* $^{flox/flox}$ and *Foxp2* $^{flox/flox}$. Both male and female mice were used in all experiments in equal numbers. All mice were located in the same room in the mouse facility and were maintained on a 12-h light on/off schedule where they were given access to food and water *ad libitum*. No difference due to sex was found and thus all animals were grouped together for analysis.

METHOD DETAILS

Data analysis for behavior and electrophysiology—For behavior data, sample number is the number of animals. An equal number of male and female mice were used for experiments. For electrophysiology, sample number is the number of neurons. All data are plotted as mean ± standard error. Unless otherwise indicated, a two-way analysis of variance (ANOVA) with Tukey's or Holm-Sidak's post-hoc multiple comparisons test was used.

Behavior

Nest building: Nests were scored as we previously published.[18] After weaning, mice were co-housed with other mice of the same sex. Once they reached >6 weeks of age, the mice were then separated and singly housed in new cages that had an intact nestlet material. Mice were then kept in the cage overnight and after approximately 18 h, the nests were scored to assess quality on a scale from 1 to 5 following an established scoring system.[87]

Rotarod: Following previously published methods, adult mice were brought to the room with the testing apparatus, weighed, and given 30 min to habituate.[18,21] They were then placed on a textured rod within individual lanes of a Series 8 IITC Life Science rotarod. The rod was programmed to accelerate from 4 to 40 rpm within a 5-min time frame. Each mouse was placed, facing forward, on the rod before starting the test. Sensors located below the rod were activated when the mouse fell off the rod. If the mouse made one full rotation holding onto the rod, the sensor was manually activated, and the mouse was taken off the rod. Once all mice in a test had completed the paradigm (maximum of 5 at a time), latency to fall and maximum revolutions per minute at fall were recorded. Mice were then placed back in their home cage, rods and sensors were cleaned with 70% ethanol, and then the next set of mice were tested. Mice of opposite sexes were not tested at the same time. Mice were tested for three consecutive days with four trials per day, separated by 10-min intervals.

Grip strength: Following previously published protocols, forelimb and hindlimb grip strength were measured at least one day after completion of the rotarod.[18,21] The Chatillon Force Measurement equipment was used to record the amount of strength it took to pull the mouse off a mesh wire. Fore (or hind) limbs of each mouse were placed onto a mesh wire meter and then pulled away using constant force. Five consecutive measurements were recorded for both forelimbs and hindlimbs. An average grip strength for both forelimbs and hindlimbs was obtained per mouse.

Neonatal ultrasonic vocalizations: USVs were recorded by isolating pups from dams at P4, P7, and P10. They were then placed into a soundproof container that was equipped with an UltraSoundGate condenser microphone. The recordings were made using Avisoft Bioacoustic software USVs were recorded for 3 min and then pups were returned to their dams.[18,21,81] Briefly, pups were isolated form and Analysis of sound spectrograms was performed using an established MATLAB script.[124]

Single-nucleus RNA-Sequencing (snRNA-Seq)

Tissue Collection and processing (P56): P56 mice were sacrificed by rapid dissection and brains were quickly removed and placed in ice-cold 1X PBS. Using a brain matrix with 1mm markings, striatal sections were obtained, as determined by visual cues indicating the presence of the striatum. Using forceps, the dorsal striatum was separated from the cortex, flash frozen, and stored in −80C. Nuclei isolation for snRNA-Seq was adapted from our own published protocols optimized for adult mouse striatum.[18,125] Briefly, tissue was homogenized in a glass Dounce tissue grinder (25 times with pestle A, 25 times with pestle B; Sigma, Cat#D8938) in 2mL ice-cold EZ Nuclei Lysis Buffer (Sigma, Cat #NUC-101). Samples were incubated on ice for 5 min with an additional 2mL ice-cold EZ lysis buffer and then centrifuged at 500 X g for 5 min at 4C, washed with 2mL ice-cold EZ lysis buffer, and incubated on ice for another 5 min before being spun again. Nuclei were then washed in 500uL Nuclei Suspension Buffer (NSB; 1X PBS, 0.01% Ultrapure BSA, and 0.1% RNase inhibitor) and mixed with 900uL nuclei sucrose cushion buffer (Sigma, Cat #NUC-201). This mixture was layered on top of another 500uL of sucrose cushion buffer and spun at 13,000 X g for 45 min at 4C. The supernatant was then discarded, the pellet was resuspended in 60uL NSB, and filtered through FLOWMI tip strainer (Bel-Art Products, Cat# H13680–0040); more NSB was added as needed to help samples go through the FLOWMI tip. An aliquot was stained with Trypan Blue and counted under a microscope to determine concentration (targeting 700–1,200 nuclei/uL). Samples were stored on ice until library generation. Libraries were prepared using the 10X Genomics Single Cell Reagent Kits v3 and v3.1 protocol targeting 10,000 nuclei total per sample.[110] A total of 12 mice (3 mice/genotype) were prepped in 5 batches. Libraries were sequenced on an Illumina NovaSeq via the McDermott Sequencing Core at UT Southwestern.

Tissue Collection and processing (P9): Striatal tissue for P9 mice was collected using our previously published methods.[18] Mice were sacrificed by rapid decapitation and brains were removed and placed in ice-cold artificial cerebrospinal fluid (ACSF; 126 mM NaCl, 20 mM NaHCO3, 20 mM D-Glucose, 3 mM KCl, 1.25 mM NaH2PO4, 2 mM CaCl2, 2 mM MgCl2) bubbled with 95% O2 and 5% CO2. 500uM coronal sections were made in ACSF using a VF-200 Compresstome (Precisionary Instruments) and transferred to another chamber filled with ACSF. From 3 dorsal striatal sections, 6 punches of striatal tissue were collected (2 per hemisphere), flash frozen, and stored in −80C. Nuclei were then isolated in a similar fashion as adults, with only one 5-min centrifugation in EZ Nuclei Lysis buffer. No sucrose cushion was used. Again, samples were filtered through the FLOWMI tip strainer, stained with Trypan Blue, counted under a microscope, and stored on ice until library generation. 12 mice were prepped in 5 batches. Libraries were sequenced as described above.

Pre-processing of sequencing data: Raw sequencing data was acquired from the McDermott Sequencing Core at UT Southwestern in the form of binary base call (BCL) files. BC files were de-multiplexed with the 10X Genomics i7 index (used during library preparation) using Illumina's bcl2fastq v2.19.1 and the *mkfastq* command from 10X Genomics CellRanger v3.0.2 suite. Resulting FASTQ files were checked for quality using FASTQC (v0.11.5).[111] A reference mouse genome-annotation index was built using mouse

genome (GRCm38p6) and Gencode annotation (vM17) with *mkref* command from 10X Genomics CellRanger v3.0.2 suite. Extracted and quality passed Extracted FASTQ reads were then aligned to reference mouse genome-annotation index and raw count tables were generated using *count* command from 10X Genomics CellRanger v3.0.2 suite. Cellbender was then run on the raw unfiltered count tables to discard potential ambient RNA.[112] Potential doublets were identified with DoubletFinder using filtered count tables generated by CellBender.[113] This produced an expression matrix containing cells as rows and genes as columns which was used for downstream analysis.

Clustering analysis: Cleaned count tables were used to run Seurat pipeline following vignette (https://satijalab.org/seurat/articles/pbmc3k_tutorial.html). Samples across genotypes were processed through Harmony to remove covariate effects such as batch and sex.[116] Harmonised Seurat objects were integrated following vignette (https://satijalab.org/seurat/articles/integration_introduction.html). Integrated data was clustered to identify clusters. Cell-type annotation was performed using known marker genes and running Fisher exact test against cell-type marker genes identified in a previous dataset.[72] Furthermore, nuclei corresponding to SPN classes were sub-clustered to resolve specific SPN sub-types (D1, D2, and eccentric SPNs) with higher granularity.

Differential gene expression analysis: For differentially expressed genes, nuclei corresponding to each SPN class were grouped by genotype. Genes with significant differential expression within D1-SPNs (or D2-or eccentric) of knockouts were identified (filtered using adjusted *p*p-value <0.05, | logFC| > 0.25) when compared to control samples using MAST-GLM.[121] Differential expression reflected changes in gene expression in SPN population across genotypes.

Gene ontology: Gene ontology of for DEGs was performed using ToppGene.[122] We used Gene Ontology and Kyto Encyclopedia of Genes and genomes databases. Expressed genes in the D1-SPNs (17,851 for juvenile and 16,542 for adult) were used as background.

Overlap with other gene databases: ASD-associated genes were downloaded from SFARI Gene database.[126] ASD (1–3) are ASD genes with a score between 1 and 3. Fragile-X associated genes were downloaded from Darnell et al. 2011.[127] Intellectual disability gene dataset was downloaded from Chen et al. 2018.[128] DEGs were overlapped with genes from each database and a Fisher's exact test was used to determine significance.

Single-nucleus assay for Transposase-accessible chromatin sequencing (snATAC-Seq): Striatal tissue from P9 mice were collected in the same manner as they were for snRNA-seq samples. Nuclei were isolated using similar methods as above but using different nuclei wash buffers specialized for ATAC-Seq (10mM Tris pH 7.4, 10mM NaCl, 3mM MgCl2, 10% BSA, and 1% Tween 20). After counting, nuclei were diluted using the 20X Nuclei Buffer (component of 10X ATAC-Seq kit) before proceeding with the 10X Genomic Single Cell ATAC Kit v1.1 and v2 protocol.[110] Between 7,000 and 10,000 nuclei were targeted per sample. A total of 12 mice (3/genotype) were prepped in 3 batches. Libraries were sequenced as described above.

Pre-processing of sequencing data: Raw BCL data for sequenced libraries were received from McDermott Sequencing Core at UT Southwestern and FASTQ files were extracted using *cellranger-atac* from 10X Genomics CellRanger-ATAC v2.0.0 suite and bcl2fastq (v2.20.0). FASTQC (v0.11.5) was run on extracted FASTQ files to check the reads quality.[111] Reference mouse genome-annotation index was built using mouse genome (GRCm38p6) and Gencode annotation (vM17) with *cellranger-atac* mkref from the 10X Genomics CellRanger-ATAC v2.0.0 suite. Fragment files were further used to identify potential doublets using ArchR (v1.0.2).[118] BAM files were converted to BED files using *bedtools bamtobed* (v2.29.2).[119] BED files were then used to call peaks using *MACS2* callpeak.[120] Using Signac (v1.9.0) and Seurat (v4.3.0), chromatin assays and Seurat objects were generated per biological replicate per genotype for shared peaks across all genotype replicates.[114,117,129] Signac pipeline was run following vignette (https://stuartlab.org/signac/articles/mouse_brain_vignette.html) to generate gene activity matrix. Individual Seurat objects processed through Signac were then filtered to remove low quality nuclei (total fragments in peaks >1,500; total fragments in peaks <100,000; percent reads in peaks >10%; nucleosome signal <2; TSS enrichment >2; blacklist ratio <0.03) and potential doublets scored by ArchR.

Clustering analysis and identification of differentially accessible regions: Samples per genotype were first merged and then processed through Harmony (v0.1.0) to remove effect of covariates such as batch and sex.[116] Harmonized Seurat objects per genotype were then integrated and data were clustered to identify clusters. Clusters were annotated using age-matched snRNA-seq data (P9) with *TransferData* function available as a part of Seurat following vignette (https://satijalab.org/seurat/articles/integration_mapping.html). Nuclei belonging to D1-SPN class were used to identify differentially accessible regions (DARs) across genotypes. Significant DARs (adjusted *pp*-value % ≤ 0.05, absolute log fold change ≥ 0.1375) were identified by comparing each knockout against control genotypes using *FindMarkers* command and likelihood ratio test (LR) following Signac vignette (https://stuartlab.org/signac/articles/mouse_brain_vignette.html). Enriched motifs were then identified for DARs following Signac's *FindMotifs* command (https://stuartlab.org/signac/articles/motif_vignette.html).[117] Motifs were determined by using the JASPAR database. All compared peaks across a pairwise comparison were used as background for motif analysis and motifs with fold enrichment >1.75 were retained.

Electrophysiological recordings: All experiments were done on mice expressing the *Drd1-tdTomato* reporter as per our previously published methods.[19] Briefly, striatal slices from P14-P18 mice were collected and recorded in nominal ACSF. Expression of tdTomato was used to identify the D1-SPNs. Current clamp recordings at incremental current steps (500 ms duration) were applied at resting potential to measure number of action potentials. In the voltage clamp, a − 10 mV voltage (500 ms duration) was applied to measure input resistance and normalized cell conductance at −85, −65, and −55 mV holding potentials. IV-plots were generated in voltage clamp conditions using a multi-step protocol (500 ms duration) ranging from −30 to −120 mV voltages at −10mV steps. Current measured was average from a 200 ms window at the end of each step.

RNA Extraction and quantitative real-time PCR (RT-qPCR): We adapted a previously published protocol to obtain single cell suspensions.[18] Briefly, mice were anesthetized and sacrificed at P14 and brains were removed and placed in ice-cold ACSF bubbled with 95% O2 and 5% CO2. 500mM coronal sections were made in ACSF and transferred to another chamber filled with ACSF. From 3 striatal sections, 6 punches of striatal tissue were collected (2 per hemisphere). Papain was added and samples were incubated at 37C for 30 min. Samples were then triturated using glass pipette. Samples were centrifuged and then resuspended in ACSF. Fluorescence-activated Cell Sorting (FACS) was used to sort D1-SPNs (marked by td-Tomato) from the remaining striatal neurons. RNA from FACS sorted cells was isolated using miRNAeasy kit guidelines. RNA was converted to cDNA using recommended guidelines from SSIII Superscript Kit (Invitrogen) and RT-qPCR was performed using the CFX384 Real-Time System (Bio-Rad). Expression of *Foxp1* and *Kcnk2* was measured from both the td-Tomato positive (D1-SPNs) and td-Tomato negative (non D1-SPN striatal cells) fractions and normalized to expression of 18S.

Immunohistochemistry, imaging, and quantification: At P56, mice were anesthetized with Euthasol and then perfused, first with 1X PBS and then by 4% PFA. Brains were then transferred into 4% PFA overnight and then to 30% sucrose with 0.01% sodium azide for at least 48 h. 50uM sagittal slices were made using a Leica 1950 cryostat and free-floating sections were stored in 1X PBS with 0.01% sodium azide. Slices were washed with 1X TBS, incubated in 3% hydrogen peroxide for 30 min, washed in 1X TBS again, and then incubated for 60 min in 0.3M glycine in 0.4% Triton X- in 1X TBS (TBS-T). Slices were washed again, this time in TBS-T and then incubated in blocking buffer (1% BSA and 3% normal donkey serum in TBS-T). Slices were then incubated in primary antibodies for two nights at 4C (antibodies diluted in blocking buffer), washed in TBS-T, and incubated in secondary antibodies (diluted in TBS-T) for 1 h at room temperature. Slices were washed again in TBS-T, incubated with diluted Hoechst solution, then mounted onto slides and allowed to dry. Sections were allowed to dry before mounting coverslips using Prolong Diamond Antifade Mountant.

Images were collected using a Zeiss Confocal laser scanning microscope (LSM880). z stack, tile images of the full brain were obtained at 20× magnification. All images were taken in similar sections across samples. Imaging was performed with the aid of The UTSW Microscopy Core and Dr. Shin Yamazaki.

Expression of Foxp1 and Foxp2 in D1-SPNs in the $Foxp1^{D1}$ and $Foxp2^{D1}$ samples was quantified by use of the Imaris cell imaging software. Briefly, images taken at 20× magnification were opened with the Imaris software and then D1-SPNs were identified by their expression of the tdTomato marker. Background noise from the images was filtered by thresholding, thereby only retaining true cells for further analysis. Surfaces detail was set to 5 and seed splitting was set to 7 μM. Intensity signal for Foxp1 and Foxp2 were similarly identified, and a minimum intensity signal was chosen for each sample. This chosen signal was used to identify the percentage of D1-SPNs expressing either Foxp1 or Foxp2. The experimenter was blinded to genotype during the quantification process. Quantification was performed with the aid of the UTSW Quantitative Light Microscopy Core and Dr. Marcel Mettlen.

Antibodies: The following primary antibodies were used for immunohistochemistry (IHC) experiments: goat anti-Foxp2 (1:500, Santa Cruz Biotechnology, cat# sc-21069), rabbit anti-Foxp1 (1:2000, validated in previous publications[18]), and rat anti-tdTomato (1:500, Kerafast, cat# EST203). The following Alexa Flour secondary antibodies were used: Alexa Flour donkey anti-rabbit 488 (Thermo Fisher, cat# A21206), donkey anti-rat 555 (Thermo Fisher cat# A78945), and donkey anti-goat 647 (Jackson ImmunoResearch cat# 711–605-152). All secondary antibodies were used at a dilution of 1:1000.

Single molecule fluorescent in situ hybridization (smFISH) and quantification: At P9, mice were euthanized, and brains were collected in OCT and snap frozen in isopentane chilled with liquid nitrogen. Brains were then sectioned at −20C to 15 μM coronal slices and thaw mounted on Superfrost Plus Microscope slides (Thermo Fisher Scientific, cat #12–550-15). Fluorescent *in situ* hybridization (FISH) was performed using RNAscope Multiplex Flourescent Reagent Kit v2 assay (Advanced Cell Diagnostics, cat# 323100) as per the manufacturer's protocol. RNAscope probes were used to identify the expression of *Ntn1* (ACD, cat# 407621), *Cdk7* (ACD, cat# 573911-C2), and *Tac1* (ACD, cat# 410351-C3). Mouse striatum was imaged in a similar fashion to what was done for immunohistochemistry. Briefly, 1 section from each of the 3 mice of each genotype was processed for RNAscope and 3–4 images were taken from every section to represent the whole striatum. ROIs were determined based on *Tac1* expression to identify D1-SPNs, and puncta for *Ntn1* and *Cdk7* were counted within the ROIs/Cells. Number of puncta within each cell were compared between control and $Foxp1^{D1}$/$Foxp2^{D1}$ mice using a Mann-Whitney's U test.

AAV-mediated injection of Foxp1: A pAAV-hSYN-Foxp1-T2A-eGFP (or control AAV9-hSYN1-eGFP construct expressing only EGFP) was injected into the striatum of mice at postnatal day 1 in litters that were expected to include $Foxp1/2^{D1}$ mice. The titers for each construct were 3.4 X 10^{12} and 2.7 X 10^{12} GC/mL respectively. Pups were anesthetized on ice and then bilateral injections were performed using a beveled glass injection pipette and a Nanoject injector (Drummond Scientific). They were then allowed to recover on a heating pad before being returned to their dams. Mice were genotyped before P14 to confirm if they were controls or $Foxp1/2^{D1}$ and whether they carried td-Tomato. Control and rescue virus injected wild type and double knockout mice that were td-Tomato positive were used for electrophysiology experiments. Neurons co-expressing td-Tomato (marking D1-SPNs) and EGFP (marking viral infected neurons) were recorded from as described earlier. Any mice not used for electrophysiology were utilized for behavioral experiments at > P56.

QUANTIFICATION AND STATISTICAL ANALYSIS

Statistical methods and code used for snRNA-seq and snATAC-seq analysis are provided in the methods section. Three animals per genotype at each time point were used. DEGs were determined using MAST-GLM and considered significant if adjusted *p*p-value <0.05 and |logFC| > 0.25 when compared to control samples. DARs were determined by comparing each knockout against control genotypes using *FindMarkers* command and likelihood ratio test (LR) and were considered significant if adjusted *p*p-value <0.05 and | logFC| > 0.1375. Peaks were compared across a pairwise comparison and used as background for motif

analysis. Motifs with fold enrichment >1.75 were considered significant. All statistical tests for behavior, electrophysiology, IHC, and smFISH were performed using GraphPad Prism to obtain *p* values and test normality. Statistical tests used for each analysis are described in depth in figure legends. Sample sizes, which were based on previously published papers, are indicated in figure legends.[18,19,81] Sample size represents number of animals in behavioral, IHC, snRNA-seq, and snATAC-seq analysis. Sample size represents the number of cells in electrophysiology and smFISH analysis. All graphs are displayed as mean ± SEM.

Supplementary Material

Refer to Web version on PubMed Central for supplementary material.

ACKNOWLEDGMENTS

Our sincerest thanks to Dr. Peter Tsai, Dr. Maria Chahrour, and Dr. Todd Roberts for providing critical feedback on the manuscript. We thank Dr. Shin Yamazaki and the Neuroscience Microscopy Facility, supported by the UTSW Neuroscience Department and the UTSW Peter O'Donnell Jr. Brain Institute. We also thank Dr. Marcel Mettlen, Dr. Katherine Phelps, and the UTSW Quantitative Light Microscopy Core for providing access to the Imaris cell-imaging software. We would like to thank Dr. Eric Plautz, Dr. Denise Ramirez, and the UTSW Neuro-Models Facility for providing access to the equipment for rotarod and grip strength. Finally, we would like to thank Dr. Benjamin Arenkiel, Dr. Joshua Ortiz, and the Baylor College of Medicine Optogenetics and Viral Design/Expression Core for designing the AAV-SYN1-FOXP1-GFP construct. G.K. is a Jon Heighten Scholar in Autism Research and Townsend Distinguished Chair in Research on Autism Spectrum Disorders at UT Southwestern. This work was supported by grants from NIMH (MH126481, MH102603), NINDS (NS126143, NS115821), the Simons Foundation (573689, 947591), and the James S. McDonnell Foundation 21st Century Science Initiative in Understanding Human Cognition – Scholar Award (220020467) to G.K. This work was further supported by the NIH/NHLBI (grant T32-HL 139438 to N.I.A.) and the NIH/NINDS (grant NS117030–01 to N.I.A.).

REFERENCES

1. Kreitzer AC, and Malenka RC (2008). Striatal plasticity and basal ganglia circuit function. Neuron 60, 543–554. 10.1016/j.neuron.2008.11.005. [PubMed: 19038213]
2. Gerfen CR, and Surmeier DJ (2011). Modulation of striatal projection systems by dopamine. Annu. Rev. Neurosci. 34, 441–466. 10.1146/annurev-neuro-061010-113641. [PubMed: 21469956]
3. Gerfen CR (1992). The neostriatal mosaic: multiple levels of compartmental organization. Trends Neurosci. 15, 133–139. [PubMed: 1374971]
4. Fuccillo MV (2016). Striatal Circuits as a Common Node for Autism Pathophysiology. Front. Neurosci. 10, 27. 10.3389/fnins.2016.00027. [PubMed: 26903795]
5. Graybiel AM, Aosaki T, Flaherty AW, and Kimura M (1994). The basal ganglia and adaptive motor control. Science 265, 1826–1831. 10.1126/science.8091209. [PubMed: 8091209]
6. Surmeier DJ, Ding J, Day M, Wang Z, and Shen W (2007). D1 and D2 dopamine-receptor modulation of striatal glutamatergic signaling in striatal medium spiny neurons. Trends Neurosci. 30, 228–235. 10.1016/j.tins.2007.03.008. [PubMed: 17408758]
7. Hachigian LJ, Carmona V, Fenster RJ, Kulicke R, Heilbut A, Sittler A, Pereira de Almeida L, Mesirov JP, Gao F, Kolaczyk ED, and Heiman M (2017). Control of Huntington's Disease-Associated Phenotypes by the Striatum-Enriched Transcription Factor Foxp2. Cell Rep. 21, 2688–2695. 10.1016/j.celrep.2017.11.018. [PubMed: 29212017]
8. Louis Sam Titus ASC, Yusuff T, Cassar M, Thomas E, Kretzschmar D, and D'Mello SR (2017). Reduced Expression of Foxp1 as a Contributing Factor in Huntington's Disease. J. Neurosci. 37, 6575–6587. 10.1523/JNEUROSCI.3612-16.2017. [PubMed: 28550168]
9. Lebouc M, Richard Q, Garret M, and Baufreton J (2020). Striatal circuit development and its alterations in Huntington's disease. Neurobiol. Dis. 145, 105076. 10.1016/j.nbd.2020.105076. [PubMed: 32898646]

10. Del Campo N, Chamberlain SR, Sahakian BJ, and Robbins TW(2011). The roles of dopamine and noradrenaline in the pathophysiology and treatment of attention-deficit/hyperactivity disorder. Biol. Psychiatry 69, e145–e157. 10.1016/j.biopsych.2011.02.036. [PubMed: 21550021]
11. Balsters JH, Mantini D, and Wenderoth N (2018). Connectivity-based parcellation reveals distinct cortico-striatal connectivity fingerprints in Autism Spectrum Disorder. Neuroimage 170, 412–423. 10.1016/j.neuroimage.2017.02.019. [PubMed: 28188914]
12. Matsushima A, Pineda SS, Crittenden JR, Lee H, Galani K, Mantero J, Tombaugh G, Kellis M, Heiman M, and Graybiel AM (2023). Transcriptional vulnerabilities of striatal neurons in human and rodent models of Huntington's disease. Nat. Commun. 14, 282. 10.1038/s41467-022-35752-x. [PubMed: 36650127]
13. Yang L, Su Z, Wang Z, Li Z, Shang Z, Du H, Liu G, Qi D, Yang Z, Xu Z, and Zhang Z (2021). Transcriptional profiling reveals the transcription factor networks regulating the survival of striatal neurons. Cell Death Dis. 12, 262. 10.1038/s41419-021-03552-8. [PubMed: 33712552]
14. Lambert SA, Jolma A, Campitelli LF, Das PK, Yin Y, Albu M, Chen X, Taipale J, Hughes TR, and Weirauch MT (2018). The Human Transcription Factors. Cell 172, 650–665. 10.1016/j.cell.2018.01.029. [PubMed: 29425488]
15. Lee TI, and Young RA (2013). Transcriptional regulation and its misregulation in disease. Cell 152, 1237–1251. 10.1016/j.cell.2013.02.014. [PubMed: 23498934]
16. Ferland RJ, Cherry TJ, Preware PO, Morrisey EE, and Walsh CA (2003). Characterization of Foxp2 and Foxp1 mRNA and protein in the developing and mature brain. J. Comp. Neurol. 460, 266–279. 10.1002/cne.10654. [PubMed: 12687690]
17. Wijchers PJEC, Hoekman MFM, Burbach JPH, and Smidt MP (2006). Identification of forkhead transcription factors in cortical and dopaminergic areas of the adult murine brain. Brain Res. 1068, 23–33. 10.1016/j.brainres.2005.11.022. [PubMed: 16376864]
18. Anderson AG, Kulkarni A, Harper M, and Konopka G (2020). Single-Cell Analysis of Foxp1-Driven Mechanisms Essential for Striatal Development. Cell Rep. 30, 3051–3066.e7. 10.1016/j.celrep.2020.02.030. [PubMed: 32130906]
19. Khandelwal N, Cavalier S, Rybalchenko V, Kulkarni A, Anderson AG, Konopka G, and Gibson JR (2021). FOXP1 negatively regulates intrinsic excitability in D2 striatal projection neurons by promoting inwardly rectifying and leak potassium currents. Mol. Psychiatry 26, 1761–1774. 10.1038/s41380-020-00995-x. [PubMed: 33402705]
20. Fong WL, Kuo HY, Wu HL, Chen SY, and Liu FC (2018). Differential and Overlapping Pattern of Foxp1 and Foxp2 Expression in the Striatum of Adult Mouse Brain. Neuroscience 388, 214–223. 10.1016/j.neuroscience.2018.07.017. [PubMed: 30031127]
21. Araujo DJ, Anderson AG, Berto S, Runnels W, Harper M, Ammanuel S, Rieger MA, Huang HC, Rajkovich K, Loerwald KW, et al. (2015). FoxP1 orchestration of ASD-relevant signaling pathways in the striatum. Genes Dev. 29, 2081–2096. 10.1101/gad.267989.115. [PubMed: 26494785]
22. Konopka G, and Roberts TF (2016). Insights into the Neural and Genetic Basis of Vocal Communication. Cell 164, 1269–1276. 10.1016/j.cell.2016.02.039. [PubMed: 26967292]
23. Li S, Weidenfeld J, and Morrisey EE (2004). Transcriptional and DNA Binding Activity of the Foxp1/2/4 Family Is Modulated by Heterotypic and Homotypic Protein Interactions. Mol. Cell Biol. 24, 809–822. 10.1128/mcb.24.2.809-822.2004. [PubMed: 14701752]
24. Deriziotis P, Graham SA, Estruch SB, and Fisher SE (2014). Investigating protein-protein interactions in live cells using bioluminescence resonance energy transfer. J. Vis. Exp. 87, 51438. 10.3791/51438.
25. Estruch SB, Graham SA, Quevedo M, Vino A, Dekkers DHW, Deriziotis P, Sollis E, Demmers J, Poot RA, and Fisher SE (2018). Proteomic analysis of FOXP proteins reveals interactions between cortical transcription factors associated with neurodevelopmental disorders. Hum. Mol. Genet. 27, 1212–1227. 10.1093/hmg/ddy035. [PubMed: 29365100]
26. Sin C, Li H, and Crawford DA (2015). Transcriptional regulation byFOXP1, FOXP2, and FOXP4 dimerization. J. Mol. Neurosci. 55, 437–448. 10.1007/s12031-014-0359-7. [PubMed: 25027557]

27. Stroud JC, Wu Y, Bates DL, Han A, Nowick K, Paabo S, Tong H, and Chen L (2006). Structure of the forkhead domain of FOXP2 bound to DNA. Structure 14, 159–166. 10.1016/j.str.2005.10.005. [PubMed: 16407075]
28. Mitsis T, Efthimiadou A, Bacopoulou F, Vlachakis D, Chrousos G, and Eliopoulos E (2020). Transcription factors and evolution: An integral part of gene expression (Review). World Acad. Sci. J. 2, 3–8. 10.3892/wasj.2020.32.
29. Amoutzias GD, Robertson DL, Van de Peer Y, and Oliver SG(2008). Choose your partners: dimerization in eukaryotic transcription factors. Trends Biochem. Sci. 33, 220–229. 10.1016/j.tibs.2008.02.002. [PubMed: 18406148]
30. Gera T, Jonas F, More R, and Barkai N (2022). Evolution of binding preferences among whole-genome duplicated transcription factors. Elife 11, e73225. 10.7554/eLife.73225. [PubMed: 35404235]
31. Majidi SP, Reddy NC, Moore MJ, Chen H, Yamada T, Andzelm MM, Cherry TJ, Hu LS, Greenberg ME, and Bonni A (2019). Chromatin Environment and Cellular Context Specify Compensatory Activity of Paralogous MEF2 Transcription Factors. Cell Rep. 29, 2001–2015.e5. 10.1016/j.celrep.2019.10.033. [PubMed: 31722213]
32. Macneil LT, and Walhout AJM (2011). Gene regulatory networks and the role of robustness and stochasticity in the control of gene expression. Genome Res. 21, 645–657. 10.1101/gr.097378.109. [PubMed: 21324878]
33. Spaeth JM, Hunter CS, Bonatakis L, Guo M, French CA, Slack I, Hara M, Fisher SE, Ferrer J, Morrisey EE, et al. (2015). The FOXP1, FOXP2 and FOXP4 transcription factors are required for islet alpha cell proliferation and function in mice. Diabetologia 58, 1836–1844. 10.1007/s00125-015-3635-3. [PubMed: 26021489]
34. Li S, Morley M, Lu M, Zhou S, Stewart K, French CA, Tucker HO, Fisher SE, and Morrisey EE (2016). Foxp transcription factors suppress a non-pulmonary gene expression program to permit proper lung development. Dev. Biol. 416, 338–346. 10.1016/j.ydbio.2016.06.020. [PubMed: 27341756]
35. Zhao H, Zhou W, Yao Z, Wan Y, Cao J, Zhang L, Zhao J, Li H,Zhou R, Li B, et al. (2015). Foxp1/2/4 regulate endochondral ossification as a suppresser complex. Dev. Biol. 398, 242–254. 10.1016/j.ydbio.2014.12.007. [PubMed: 25527076]
36. Shu W, Lu MM, Zhang Y, Tucker PW, Zhou D, and Morrisey EE (2007). Foxp2 and Foxp1 cooperatively regulate lung and esophagus development. Development 134, 1991–2000. 10.1242/dev.02846. [PubMed: 17428829]
37. Co M, Anderson AG, and Konopka G (2020). FOXP transcription factors in vertebrate brain development, function, and disorders. Wiley Interdiscip. Rev. Dev. Biol. 9, e375. 10.1002/wdev.375. [PubMed: 31999079]
38. Precious SV, Kelly CM, Reddington AE, Vinh NN, Stickland RC, Pekarik V, Scherf C, Jeyasingham R, Glasbey J, Holeiter M, et al. (2016). FoxP1 marks medium spiny neurons from precursors to maturity and is required for their differentiation. Exp. Neurol. 282, 9–18. 10.1016/j.expneurol.2016.05.002. [PubMed: 27154297]
39. Chen YC, Kuo HY, Bornschein U, Takahashi H, Chen SY, Lu KM, Yang HY, Chen GM, Lin JR, Lee YH, et al. (2016). Foxp2 controls synaptic wiring of corticostriatal circuits and vocal communication by opposing Mef2c. Nat. Neurosci. 19, 1513–1522. 10.1038/nn.4380. [PubMed: 27595386]
40. Schreiweis C, Bornschein U, Burguière E, Kerimoglu C, Schreiter S, Dannemann M, Goyal S, Rea E, French CA, Puliyadi R, et al. (2014). Humanized Foxp2 accelerates learning by enhancing transitions from declarative to procedural performance. Proc. Natl. Acad. Sci. USA 111, 14253–14258. 10.1073/pnas.1414542111. [PubMed: 25225386]
41. Enard W, Gehre S, Hammerschmidt K, Hölter SM, Blass T, Somel M, Brückner MK, Schreiweis C, Winter C, Sohr R, et al. (2009). A humanized version of Foxp2 affects cortico-basal ganglia circuits in mice. Cell 137, 961–971. 10.1016/j.cell.2009.03.041. [PubMed: 19490899]
42. Reimers-Kipping S, Hevers W, Pääbo S, and Enard W (2011). Humanized Foxp2 specifically affects cortico-basal ganglia circuits. Neuroscience 175, 75–84. 10.1016/j.neuroscience.2010.11.042. [PubMed: 21111790]

43. Enard W (2011). FOXP2 and the role of cortico-basal ganglia circuits in speech and language evolution. Curr. Opin. Neurobiol. 21, 415–424. 10.1016/j.conb.2011.04.008. [PubMed: 21592779]
44. Satterstrom FK, Kosmicki JA, Wang J, Breen MS, De Rubeis S, An JY, Peng M, Collins R, Grove J, Klei L, et al. (2020). Large-Scale Exome Sequencing Study Implicates Both Developmental and Functional Changes in the Neurobiology of Autism. Cell 180, 568–584.e23. 10.1016/j.cell.2019.12.036. [PubMed: 31981491]
45. Zhou X, Feliciano P, Shu C, Wang T, Astrovskaya I, Hall JB, Obiajulu JU, Wright JR, Murali SC, Xu SX, et al. (2022). Integrating de novo and inherited variants in 42,607 autism cases identifies mutations in new moderate-risk genes. Nat. Genet. 54, 1305–1319. 10.1038/s41588-022-01148-2. [PubMed: 35982159]
46. Alenezi S, Alyahya A, and Aldhalaan H (2021). Autism Spectrum Disorder (ASD) and Attention Deficit Hyperactivity Disorder (ADHD) With Language Impairment Accompanied by Developmental Disability Caused by Forkhead Box Protein 1 (FOXP1) Exon Deletion: A Case Report. Cureus 13, e20595. 10.7759/cureus.20595. [PubMed: 35103171]
47. Trost B, Thiruvahindrapuram B, Chan AJS, Engchuan W, Higginbotham EJ, Howe JL, Loureiro LO, Reuter MS, Roshandel D, Whitney J, et al. (2022). Genomic architecture of autism from comprehensive whole-genome sequence annotation. Cell 185, 4409–4427.e18. 10.1016/j.cell.2022.10.009. [PubMed: 36368308]
48. Lai CS, Fisher SE, Hurst JA, Vargha-Khadem F, and Monaco AP (2001). A forkhead-domain gene is mutated in a severe speech and langauge disorder. Nature 413, 519–523. [PubMed: 11586359]
49. Siper PM, De Rubeis S, Trelles MDP, Durkin A, Di Marino D, Muratet F, Frank Y, Lozano R, Eichler EE, Kelly M, et al. (2017). Prospective investigation of FOXP1 syndrome. Mol. Autism. 8, 57. 10.1186/s13229-017-0172-6. [PubMed: 29090079]
50. Sollis E, Deriziotis P, Saitsu H, Miyake N, Matsumoto N, Hoffer MJV, Ruivenkamp CAL, Alders M, Okamoto N, Bijlsma EK, et al. (2017). Equivalent missense variant in the FOXP2 and FOXP1 transcription factors causes distinct neurodevelopmental disorders. Hum. Mutat. 38, 1542–1554. 10.1002/humu.23303. [PubMed: 28741757]
51. Sollis E, Graham SA, Vino A, Froehlich H, Vreeburg M, Dimitropoulou D, Gilissen C, Pfundt R, Rappold GA, Brunner HG, et al. (2016). Identification and functional characterization of de novo FOXP1 variants provides novel insights into the etiology of neurodevelopmental disorder. Hum. Mol. Genet. 25, 546–557. 10.1093/hmg/ddv495. [PubMed: 26647308]
52. Bacon C, and Rappold GA (2012). The distinct and overlapping phenotypic spectra of FOXP1 and FOXP2 in cognitive disorders. Hum. Genet. 131, 1687–1698. 10.1007/s00439-012-1193-z. [PubMed: 22736078]
53. Bacon C, Schneider M, Le Magueresse C, Froehlich H, Sticht C, Gluch C, Monyer H, and Rappold GA (2015). Brain-specific Foxp1 deletion impairs neuronal development and causes autistic-like behaviour. Mol. Psychiatry 20, 632–639. 10.1038/mp.2014.116. [PubMed: 25266127]
54. Spiteri E, Konopka G, Coppola G, Bomar J, Oldham M, Ou J,Vernes SC, Fisher SE, Ren B, and Geschwind DH (2007). Identification of the transcriptional targets of FOXP2, a gene linked to speech and language, in developing human brain. Am. J. Hum. Genet. 81, 1144–1157. 10.1086/522237. [PubMed: 17999357]
55. Konopka G, and Roberts TF (2016). Animal Models of Speech and Vocal Communication Deficits Associated With Psychiatric Disorders. Biol. Psychiatry 79, 53–61. 10.1016/j.biopsych.2015.07.001. [PubMed: 26232298]
56. Tierney C, Mayes S, Lohs SR, Black A, Gisin E, and Veglia M (2015). How Valid Is the Checklist for Autism Spectrum Disorder When a Child Has Apraxia of Speech? J. Dev. Behav. Pediatr. 36, 569–574. 10.1097/dbp.0000000000000189. [PubMed: 26114615]
57. Vernes SC, Nicod J, Elahi FM, Coventry JA, Kenny N, Coupe AM, Bird LE, Davies KE, and Fisher SE (2006). Functional genetic analysis of mutations implicated in a human speech and language disorder. Hum. Mol. Genet. 15, 3154–3167. 10.1093/hmg/ddl392. [PubMed: 16984964]
58. Vernes SC, Spiteri E, Nicod J, Groszer M, Taylor JM, Davies KE,Geschwind DH, and Fisher SE (2007). High-throughput analysis of promoter occupancy reveals direct neural targets of FOXP2, a gene mutated in speech and language disorders. Am. J. Hum. Genet. 81, 1232–1250. 10.1086/522238. [PubMed: 17999362]

59. MacDermot KD, Bonora E, Sykes N, Coupe AM, Lai CSL, Vernes SC, Vargha-Khadem F, McKenzie F, Smith RL, Monaco AP, and Fisher SE (2005). Identification of FOXP2 truncation as a novel cause of developmental speech and language deficits. Am. J. Hum. Genet. 76, 1074–1080. 10.1086/430841. [PubMed: 15877281]
60. Braden RO, Amor DJ, Fisher SE, Mei C, Myers CT, Mefford H, Gill D, Srivastava S, Swanson LC, Goel H, et al. (2021). Severe speech impairment is a distinguishing feature of FOXP1-related disorder. Dev. Med. Child Neurol. 63, 1417–1426. 10.1111/dmcn.14955. [PubMed: 34109629]
61. Morison LD, Meffert E, Stampfer M, Steiner-Wilke I, Vollmer B, Schulze K, Briggs T, Braden R, Vogel A, Thompson-Lake D, et al. (2023). In-depth characterisation of a cohort of individuals with missense and loss-of-function variants disrupting FOXP2. J. Med. Genet. 60, 597–607. 10.1136/jmg-2022-108734. [PubMed: 36328423]
62. Fisher SE, Vargha-Khadem F, Watkins KE, Monaco AP, and Pembrey ME (1998). Localisation of a gene implicated in a severe speech and language disorder. Nat. Genet. 18, 168–170. 10.1038/ng0298-168. [PubMed: 9462748]
63. Zilina O, Reimand T, Zjablovskaja P, Mä nnik K, Männamaa M, Traat A, Puusepp-Benazzouz H, Kurg A, and Ounap K (2012). Maternally and paternally inherited deletion of 7q31 involving the FOXP2 gene in two families. Am. J. Med. Genet. 158a, 254–256. 10.1002/ajmg.a.34378. [PubMed: 22105961]
64. Trelles MP, Levy T, Lerman B, Siper P, Lozano R, Halpern D, Walker H, Zweifach J, Frank Y, Foss-Feig J, et al. (2021). Individuals with FOXP1 syndrome present with a complex neurobehavioral profile with high rates of ADHD, anxiety, repetitive behaviors, and sensory symptoms. Mol. Autism. 12, 61. 10.1186/s13229-021-00469-z. [PubMed: 34588003]
65. Clyde D (2019). Risk loci for ADHD. Nat. Rev. Genet. 20, 69. 10.1038/s41576-018-0084-0. [PubMed: 30532079]
66. Sánchez-Morán M, Hernández JA, Duñabeitia JA, Estévez A, Bárcena L, González-Lahera A, Bajo MT, Fuentes LJ, Aransay AM, and Carreiras M (2018). Genetic association study of dyslexia and ADHD candidate genes in a Spanish cohort: Implications of comorbid samples. PLoS One 13, e0206431. 10.1371/journal.pone.0206431. [PubMed: 30379906]
67. Meyer GP, da Silva BS, Bandeira CE, Tavares MEA, Cupertino RB, Oliveira EP, Müller D, Kappel DB, Teche SP, Vitola ES, et al. (2023). Dissecting the cross-trait effects of the FOXP2 GWAS hit on clinical and brain phenotypes in adults with ADHD. Eur. Arch. Psychiatry Clin. Neurosci. 273, 15–24. 10.1007/s00406-022-01388-7. [PubMed: 35279744]
68. Demontis D, Walters GB, Athanasiadis G, Walters R, Therrien K, Nielsen TT, Farajzadeh L, Voloudakis G, Bendl J, Zeng B, et al. (2023). Genome-wide analyses of ADHD identify 27 risk loci, refine the genetic architecture and implicate several cognitive domains. Nat. Genet. 55, 198–208. 10.1038/s41588-022-01285-8. [PubMed: 36702997]
69. French CA, Vinueza Veloz MF, Zhou K, Peter S, Fisher SE, Costa RM, and De Zeeuw CI (2019). Differential effects of Foxp2 disruption in distinct motor circuits. Mol. Psychiatry 24, 447–462. 10.1038/s41380-018-0199-x. [PubMed: 30108312]
70. Rousso DL, Pearson CA, Gaber ZB, Miquelajauregui A, Li S, Portera-Cailliau C, Morrisey EE, and Novitch BG (2012). Foxp-Mediated Suppression of N-Cadherin Regulates Neuroepithelial Character and Progenitor Maintenance in the CNS. Neuron 74, 314–330. 10.1016/j.neuron.2012.02.024. [PubMed: 22542185]
71. Kaestner KH, Knochel W, and Martinez DE (2000). Unified nomenclature for the winged helix/forkhead transcription factors. Genes Dev. 14, 142–146. [PubMed: 10702024]
72. Saunders A, Macosko EZ, Wysoker A, Goldman M, Krienen FM, de Rivera H, Bien E, Baum M, Bortolin L, Wang S, et al. (2018). Molecular Diversity and Specializations among the Cells of the Adult Mouse Brain. Cell 174, 1015–1030.e16. 10.1016/j.cell.2018.07.028. [PubMed: 30096299]
73. Hickey SL, Berto S, and Konopka G (2019). Chromatin Decondensation by FOXP2 Promotes Human Neuron Maturation and Expression of Neurodevelopmental Disease Genes. Cell Rep. 27, 1699–1711.e9. 10.1016/j.celrep.2019.04.044. [PubMed: 31067457]
74. Takahashi K, Liu FC, Hirokawa K, and Takahashi H (2008). Expression of Foxp4 in the developing and adult rat forebrain. J. Neurosci. Res. 86, 3106–3116. 10.1002/jnr.21770. [PubMed: 18561326]

75. Waclaw RR, Ehrman LA, Merchan-Sala P, Kohli V, Nardini D, and Campbell K (2017). Foxo1 is a downstream effector of Isl1 in direct pathway striatal projection neuron development within the embryonic mouse telencephalon. Mol. Cell. Neurosci. 80, 44–51. 10.1016/j.mcn.2017.02.003. [PubMed: 28213137]
76. Hoekman MFM, Jacobs FMJ, Smidt MP, and Burbach JPH (2006). Spatial and temporal expression of FoxO transcription factors in the developing and adult murine brain. Gene Expr. Patterns 6, 134–140. 10.1016/j.modgep.2005.07.003. [PubMed: 16326148]
77. Wang J, Fröhlich H, Torres FB, Silva RL, Poschet G, Agarwal A, and Rappold GA (2022). Mitochondrial dysfunction and oxidative stress contribute to cognitive and motor impairment in FOXP1 syndrome. Proc Natl Acad Sci USA 119. 10.1073/pnas.2112852119.
78. Neyroud D, Nosacka RL, Callaway CS, Trevino JG, Hu H, Judge SM, and Judge AR (2021). FoxP1 is a transcriptional repressor associated with cancer cachexia that induces skeletal muscle wasting and weakness. J. Cachexia Sarcopenia Muscle 12, 421–442. 10.1002/jcsm.12666. [PubMed: 33527776]
79. Yu L, Moshelion M, and Moran N (2001). Extracellular protons inhibit the activity of inward-rectifying potassium channels in the motor cells of Samanea saman pulvini. Plant Physiol. 127, 1310–1322. [PubMed: 11706209]
80. Yao Z, van Velthoven CTJ, Nguyen TN, Goldy J, Sedeno-Cortes AE, Baftizadeh F, Bertagnolli D, Casper T, Chiang M, Crichton K, et al. (2021). A taxonomy of transcriptomic cell types across the isocortex and hippocampal formation. Cell 184, 3222–3241.e26. 10.1016/j.cell.2021.04.021. [PubMed: 34004146]
81. Araujo DJ, Toriumi K, Escamilla CO, Kulkarni A, Anderson AG, Harper M, Usui N, Ellegood J, Lerch JP, Birnbaum SG, et al. (2017). Foxp1 in Forebrain Pyramidal Neurons Controls Gene Expression Required for Spatial Learning and Synaptic Plasticity. J. Neurosci. 37, 10917–10931. 10.1523/JNEUROSCI.1005-17.2017. [PubMed: 28978667]
82. French CA, Jin X, Campbell TG, Gerfen E, Groszer M, Fisher SE, and Costa RM (2012). An aetiological Foxp2 mutation causes aberrant striatal activity and alters plasticity during skill learning. Mol. Psychiatry 17, 1077–1085. 10.1038/mp.2011.105. [PubMed: 21876543]
83. Frohlich H, Rafiullah R, Schmitt N, Abele S, and Rappold GA (2017). Foxp1 expression is essential for sex-specific murine neonatal ultrasonic vocalization. Hum. Mol. Genet. 26, 1511–1521. 10.1093/hmg/ddx055. [PubMed: 28204507]
84. Herrero MJ, Wang L, Hernandez-Pineda D, Banerjee P, Matos HY, Goodrich M, Panigrahi A, Smith NA, and Corbin JG (2021). Sex-Specific Social Behavior and Amygdala Proteomic Deficits in Foxp2 (+/−) Mutant Mice. Front. Behav. Neurosci. 15, 706079. 10.3389/fnbeh.2021.706079. [PubMed: 34421555]
85. Medvedeva VP, Rieger MA, Vieth B, Mombereau C, Ziegenhain C, Ghosh T, Cressant A, Enard W, Granon S, Dougherty JD, and Groszer M (2019). Altered social behavior in mice carrying a cortical Foxp2 deletion. Hum. Mol. Genet. 28, 701–717. 10.1093/hmg/ddy372. [PubMed: 30357341]
86. Co M, Hickey SL, Kulkarni A, Harper M, and Konopka G (2020). Cortical Foxp2 Supports Behavioral Flexibility and Developmental Dopamine D1 Receptor Expression. Cereb. Cortex 30, 1855–1870. 10.1093/cercor/bhz209. [PubMed: 31711176]
87. Deacon RMJ (2006). Assessing nest building in mice. Nat. Protoc. 1, 1117–1119. 10.1038/nprot.2006.170. [PubMed: 17406392]
88. Samidurai A, Xi L, Das A, Iness AN, Vigneshwar NG, Li PL, Singla DK, Muniyan S, Batra SK, and Kukreja RC (2021). Role of phosphodiesterase 1 in the pathophysiology of diseases and potential therapeutic opportunities. Pharmacol. Ther. 226, 107858. 10.1016/j.pharmthera.2021.107858. [PubMed: 33895190]
89. Veale EL, Golluscio A, Grand K, Graham JM, and Mathie A (2022). A KCNB1 gain of function variant causes developmental delay and speech apraxia but not seizures. Front. Pharmacol. 13, 1093313. 10.3389/fphar.2022.1093313. [PubMed: 36618935]
90. Chen Q, Heston JB, Burkett ZD, and White SA (2013). Expression analysis of the speech-related genes FoxP1 and FoxP2 and their relation to singing behavior in two songbird species. J. Exp. Biol. 216, 3682–3692. 10.1242/jeb.085886. [PubMed: 24006346]

91. Wohlgemuth S, Adam I, and Scharff C (2014). FoxP2 in songbirds. Curr. Opin. Neurobiol. 28, 86–93. 10.1016/j.conb.2014.06.009. [PubMed: 25048597]
92. Hilliard AT, Miller JE, Fraley ER, Horvath S, and White SA (2012). Molecular microcircuitry underlies functional specification in a basal ganglia circuit dedicated to vocal learning. Neuron 73, 537–552. 10.1016/j.neuron.2012.01.005. [PubMed: 22325205]
93. Guang S, Pang N, Deng X, Yang L, He F, Wu L, Chen C, Yin F, and Peng J (2018). Synaptopathology Involved in Autism Spectrum Disorder. Front. Cell. Neurosci. 12, 470. 10.3389/fncel.2018.00470. [PubMed: 30627085]
94. Cuttler K, Hassan M, Carr J, Cloete R, and Bardien S (2021). Emerging evidence implicating a role for neurexins in neurodegenerative and neuropsychiatric disorders. Open Biol. 11, 210091. 10.1098/rsob.210091. [PubMed: 34610269]
95. Davatolhagh MF, and Fuccillo MV (2021). Neurexin1 differentially regulates synaptic efficacy within striatal circuits. Cell Rep. 34, 108773. 10.1016/j.celrep.2021.108773. [PubMed: 33626349]
96. Alabi OO, Davatolhagh MF, Robinson M, Fortunato MP, Vargas Cifuentes L, Kable JW, and Fuccillo MV (2020). Disruption of Nrxn1α within excitatory forebrain circuits drives value-based dysfunction. Elife 9, e54838. 10.7554/eLife.54838. [PubMed: 33274715]
97. Gurevich EV, Gainetdinov RR, and Gurevich VV (2016). G protein-coupled receptor kinases as regulators of dopamine receptor functions. Pharmacol. Res. 111, 1–16. 10.1016/j.phrs.2016.05.010. [PubMed: 27178731]
98. Pierce KL, Premont RT, and Lefkowitz RJ (2002). Seven-transmembrane receptors. Nat. Rev. Mol. Cell Biol. 3, 639–650. 10.1038/nrm908. [PubMed: 12209124]
99. Zhuang X, Belluscio L, and Hen R (2000). G(olf)alpha mediates dopamine D1 receptor signaling. J. Neurosci. 20, Rc91. 10.1523/JNEUROSCI.20-16-j0001.2000. [PubMed: 10924528]
100. Corvol JC, Studler JM, Schonn JS, Girault JA, and Hervé D (2001). Galpha(olf) is necessary for coupling D1 and A2a receptors to adenylyl cyclase in the striatum. J. Neurochem. 76, 1585–1588. 10.1046/j.1471-4159.2001.00201.x. [PubMed: 11238742]
101. Boczek T, Mackiewicz J, Sobolczyk M, Wawrzyniak J, Lisek M, Ferenc B, Guo F, and Zylinska L (2021). The Role of G Protein-Coupled Receptors (GPCRs) and Calcium Signaling in Schizophrenia. Focus on GPCRs Activated by Neurotransmitters and Chemokines. Cells 10, 1228. [PubMed: 34067760]
102. Stratakis CA (2012). Cyclic AMP, protein kinase A, and phosphodiesterases: proceedings of an international workshop. Horm. Metab. Res. 44, 713–715. 10.1055/s-0031-1301327. [PubMed: 22951901]
103. Rex EB, Rankin ML, Ariano MA, and Sibley DR (2008). Ethanol regulation of D(1) dopamine receptor signaling is mediated by protein kinase C in an isozyme-specific manner. Neuropsychopharmacology 33, 2900–2911. 10.1038/npp.2008.16. [PubMed: 18288091]
104. Rankin ML, and Sibley DR (2010). Constitutive phosphorylation by protein kinase C regulates D1 dopamine receptor signaling. J. Neurochem. 115, 1655–1667. 10.1111/j.1471-4159.2010.07074.x. [PubMed: 20969574]
105. Iwamoto T, Okumura S, Iwatsubo K, Kawabe JI, Ohtsu K, Sakai I, Hashimoto Y, Izumitani A, Sango K, Ajiki K, et al. (2003). Motor dysfunction in type 5 adenylyl cyclase-null mice. J. Biol. Chem. 278, 16936–16940. 10.1074/jbc.C300075200. [PubMed: 12665504]
106. Kuo H-Y, Chen S-Y, Huang R-C, Takahashi H, Lee Y-H, Pang H-Y, Wu C-H, Graybiel AM, and Liu F-C (2023). Speech- and language-linked FOXP2 mutation targets protein motors in striatal neurons. Brain 146, 3542–3557. 10.1093/brain/awad090. [PubMed: 37137515]
107. Bartosovic M, Kabbe M, and Castelo-Branco G (2021). Single-cell CUT&Tag profiles histone modifications and transcription factors in complex tissues. Nat. Biotechnol. 39, 825–835. 10.1038/s41587-021-00869-9. [PubMed: 33846645]
108. Keaveney MK, Tseng HA, Ta TL, Gritton HJ, Man HY, and Han X (2018). A MicroRNA-Based Gene-Targeting Tool for Virally Labeling Interneurons in the Rodent Cortex. Cell Rep. 24, 294–303. 10.1016/j.celrep.2018.06.049. [PubMed: 29996091]
109. Ade KK, Wan Y, Chen M, Gloss B, and Calakos N (2011). An Improved BAC Transgenic Fluorescent Reporter Line for Sensitive and Specific Identification of Striatonigral Medium Spiny Neurons. Front. Syst. Neurosci. 5, 32. 10.3389/fnsys.2011.00032. [PubMed: 21713123]

110. Zheng GXY, Terry JM, Belgrader P, Ryvkin P, Bent ZW, Wilson R, Ziraldo SB, Wheeler TD, McDermott GP, Zhu J, et al. (2017). Massively parallel digital transcriptional profiling of single cells. Nat. Commun. 8, 14049. 10.1038/ncomms14049. [PubMed: 28091601]

111. Andrews S (2010). FastQC: A Quality Control Tool for High Throughput Sequence Data. https://www.bioinformatics.babraham.ac.uk/projects/fastqc/.

112. Fleming SJ, Chaffin MD, Arduini A, Akkad A-D, Banks E, Marioni JC, Philippakis AA, Ellinor PT, and Babadi M (2022). Unsupervised removal of systematic background noise from droplet-based single-cell experiments using CellBender</kbd&gt. Preprint at bioRxiv, 791699. 10.1101/791699.

113. McGinnis CS, Murrow LM, and Gartner ZJ (2019). DoubletFinder: Doublet Detection in Single-Cell RNA Sequencing Data Using Artificial Nearest Neighbors. Cell Syst. 8, 329–337.e4. 10.1016/j.cels.2019.03.003. [PubMed: 30954475]

114. Stuart T, Butler A, Hoffman P, Hafemeister C, Papalexi E, Mauck WM 3rd, Hao Y, Stoeckius M, Smibert P, and Satija R (2019). Comprehensive Integration of Single-Cell Data. Cell 177, 1888–1902.e21. 10.1016/j.cell.2019.05.031. [PubMed: 31178118]

115. Butler A, Hoffman P, Smibert P, Papalexi E, and Satija R (2018). Integrating single-cell transcriptomic data across different conditions, technologies, and species. Nat. Biotechnol. 36, 411–420. 10.1038/nbt.4096. [PubMed: 29608179]

116. Korsunsky I, Millard N, Fan J, Slowikowski K, Zhang F, Wei K, Baglaenko Y, Brenner M, Loh P. r., and Raychaudhuri S (2019). Fast, sensitive and accurate integration of single-cell data with Harmony. Nat. Methods 16, 1289–1296. 10.1038/s41592-019-0619-0. [PubMed: 31740819]

117. Stuart T, Srivastava A, Madad S, Lareau CA, and Satija R (2021). Single-cell chromatin state analysis with Signac. Nat. Methods 18, 1333–1341. 10.1038/s41592-021-01282-5. [PubMed: 34725479]

118. Granja JM, Corces MR, Pierce SE, Bagdatli ST, Choudhry H, Chang HY, and Greenleaf WJ (2021). ArchR is a scalable software package for integrative single-cell chromatin accessibility analysis. Nat. Genet. 53, 403–411. 10.1038/s41588-021-00790-6. [PubMed: 33633365]

119. Quinlan AR, and Hall IM (2010). BEDTools: a flexible suite of utilities for comparing genomic features. Bioinformatics 26, 841–842. 10.1093/bioinformatics/btq033. [PubMed: 20110278]

120. Zhang Y, Liu T, Meyer CA, Eeckhoute J, Johnson DS, Bernstein BE, Nusbaum C, Myers RM, Brown M, Li W, and Liu XS (2008). Model-based Analysis of ChIP-Seq (MACS). Genome Biol. 9, R137. 10.1186/gb-2008-9-9-r137. [PubMed: 18798982]

121. Finak G, McDavid A, Yajima M, Deng J, Gersuk V, Shalek AK, Slichter CK, Miller HW, McElrath MJ, Prlic M, et al. (2015). MAST: a flexible statistical framework for assessing transcriptional changes and characterizing heterogeneity in single-cell RNA sequencing data. Genome Biol. 16, 278. 10.1186/s13059-015-0844-5. [PubMed: 26653891]

122. Chen J, Bardes EE, Aronow BJ, and Jegga AG (2009). ToppGene Suite for gene list enrichment analysis and candidate gene prioritization. Nucleic Acids Res. 37, W305–W311. 10.1093/nar/gkp427. [PubMed: 19465376]

123. French CA, Groszer M, Preece C, Coupe AM, Rajewsky K, and Fisher SE (2007). Generation of mice with a conditional Foxp2 null allele. Genesis 45, 440–446. 10.1002/dvg.20305. [PubMed: 17619227]

124. Rieger MA, and Dougherty JD (2016). Analysis of within Subjects Variability in Mouse Ultrasonic Vocalization: Pups Exhibit Inconsistent, State-Like Patterns of Call Production. Front. Behav. Neurosci. 10, 182. 10.3389/fnbeh.2016.00182. [PubMed: 27733819]

125. Ayhan F, Kulkarni A, Berto S, Sivaprakasam K, Douglas C, Lega BC, and Konopka G (2021). Resolving cellular and molecular diversity along the hippocampal anterior-to-posterior axis in humans. Neuron 109, 2091–2105.e6. 10.1016/j.neuron.2021.05.003. [PubMed: 34051145]

126. Banerjee-Basu S, and Packer A (2010). SFARI Gene: an evolving database for the autism research community. Dis. Model. Mech. 3, 133–135. 10.1242/dmm.005439. [PubMed: 20212079]

127. Darnell JC, Van Driesche SJ, Zhang C, Hung KYS, Mele A, Fraser CE, Stone EF, Chen C, Fak JJ, Chi SW, et al. (2011). FMRP stalls ribosomal translocation on mRNAs linked to synaptic function and autism. Cell 146, 247–261. 10.1016/j.cell.2011.06.013. [PubMed: 21784246]

128. Chen C, Chen D, Xue H, Liu X, Zhang T, Tang S, Li W, and Xu X (2018). IDGenetics: a comprehensive database for genes and mutations of intellectual disability related disorders. Neurosci. Lett. 685, 96–101. 10.1016/j.neulet.2018.08.027. [PubMed: 30144540]

129. Stuart T, and Satija R (2019). Integrative single-cell analysis. Nat. Rev. Genet. 20, 257–272. 10.1038/s41576-019-0093-7. [PubMed: 30696980]

Highlights

- Combined loss of Foxp1 and Foxp2 from D1-SPNs impairs motor and social behaviors in mice
- Foxp1 and Foxp2 synergistically mediate D1-SPN excitability
- Hundreds of genes in D1-SPNs are cooperatively regulated by both Foxp1 and Foxp2
- Viral re-expression of Foxp1 is sufficient to rescue phenotypes in double knockouts

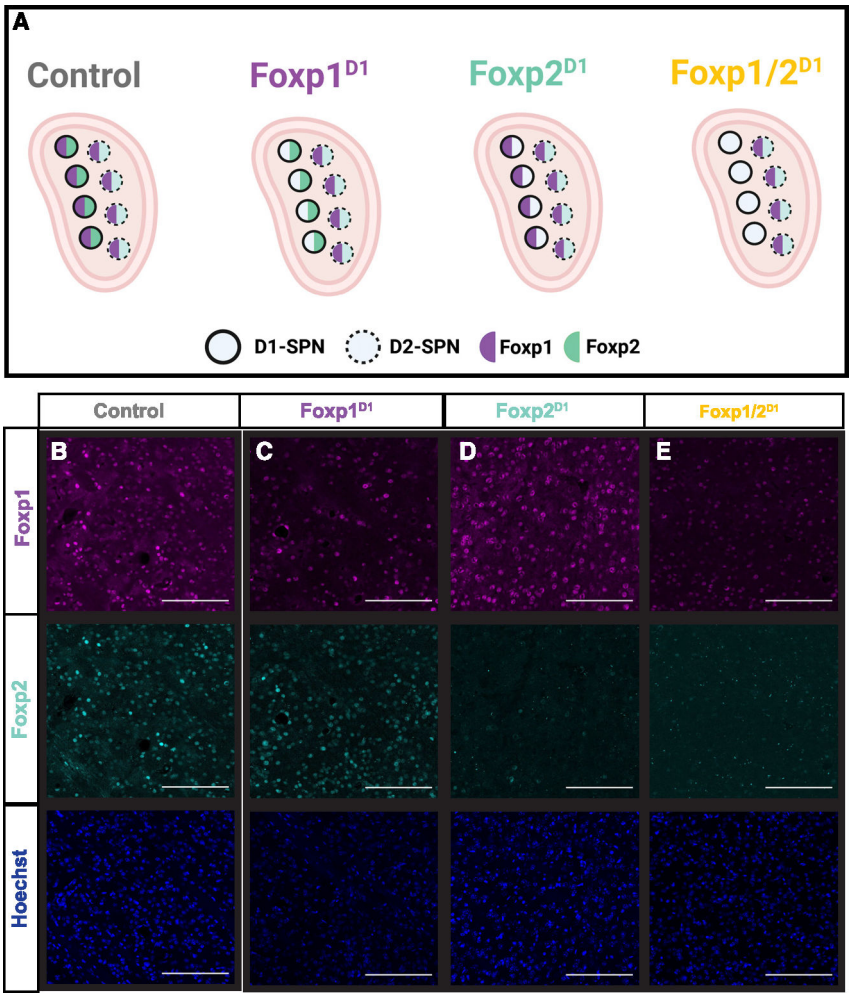

Figure 1. Validation of conditional knockouts

(A) Schematic showing the genotypes used in this study. D1-cre-mediated loss of *Foxp1* (Foxp1^{D1}; purple), *Foxp2* (Foxp2^{D1}; cyan), or both (Foxp1/2^{D1}; gold), as well as Cre-negative controls (gray).

(B–E) Representative images of immunohistochemistry for Foxp1, Foxp2, and Hoechst in control (B), Foxp1^{D1} (C), Foxp2^{D1} (D), and Foxp1/2^{D1} (E). All images from P56 mice. Scale bars represent 750 μM. 20× magnification.

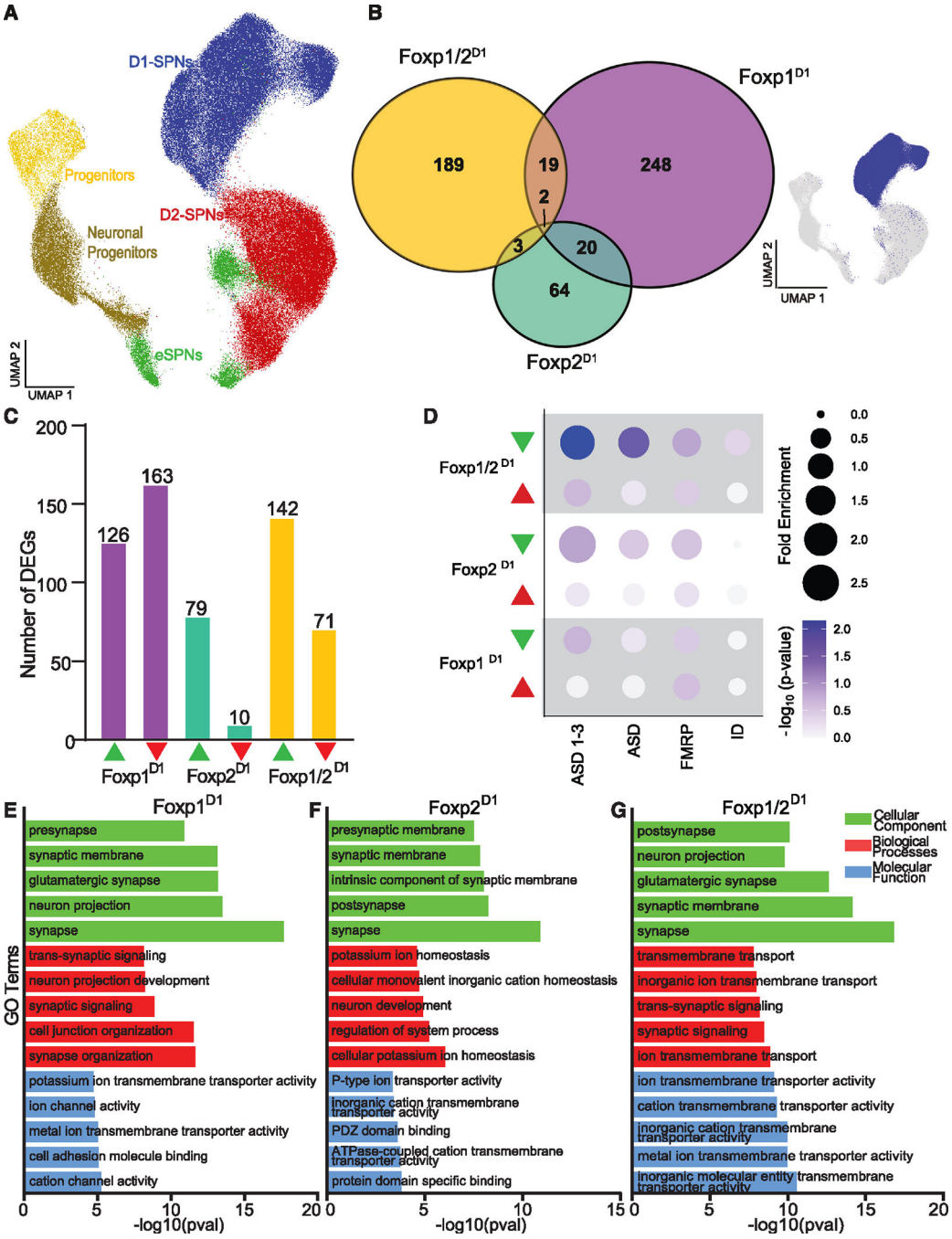

Figure 2. Loss of both *Foxp1* and *Foxp2* results in amplified loss of transcriptional regulation in D1-SPNs in juvenile mice

(A) UMAP of the neuron-only subset with colors indicating the different annotated cell types. D1-SPNs were used for DEG analysis. Genes were called differentially expressed if they had an adjusted *p* value <0.05 and logFC > |0.25|.

(B) Semi-scaled Venn diagram showing number of unique and overlapping DEGs in each knockout condition in the D1-SPNs. Overlap of DEGs between conditions was assessed by a Fisher's exact test enrichment.

(C) Bar plots showing the number of up- and downregulated genes in each knockout condition.

(D) Bubble chart showing enrichment of DEGs from each knockout condition. The $-\log_{10}(p$ value) for each enrichment is also indicated. ASD, SFARI ASD-risk genes; ASD 1–3, SFARI ASD-risk genes with scores of 1–3; FMRP, fragile X syndrome; ID, intellectual disability.

(E–G) GO analysis of (E) Foxp1^{D1}, (F) Foxp2^{D1}, and (G) Foxp1/2^{D1} DEGs reveals enrichment for terms associated with electrophysiological properties and synaptic properties.

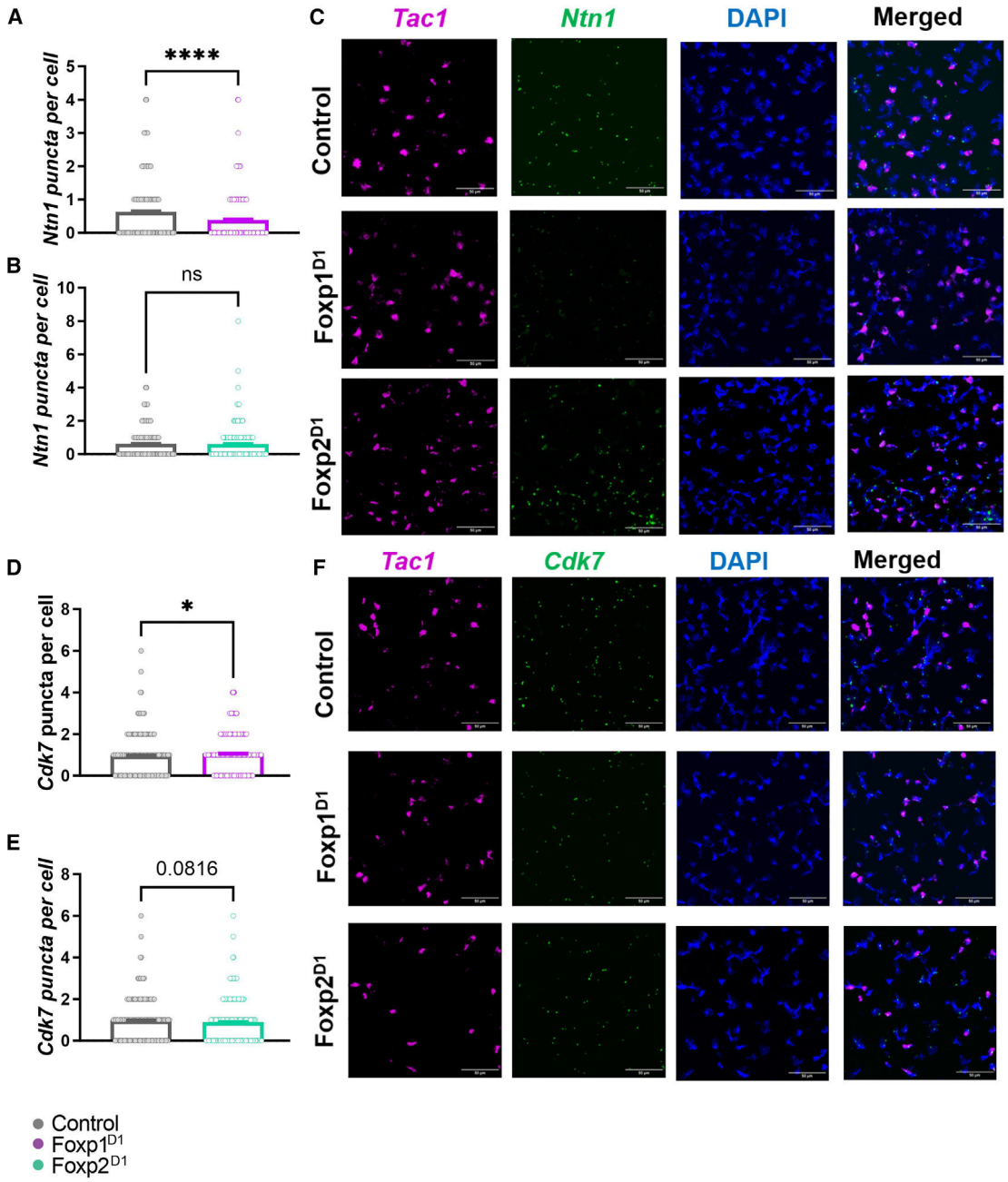

Figure 3. Validation of DEGs in single knockouts using smFISH

(A) *Ntn1* showed a downregulated expression in *Foxp1*^{D1} D1-SPNs. (B) This decrease is not in *Foxp2*^{D1} D1-SPNs. (C) Regions of interest (ROI) used to identify D1 SPNs (based on *Tac1* expression) and puncta for *Ntn1* transcripts were counted in each ROI from each each image. (D) *Cdk7* also showed a reduced expression in *Foxp1*^{D1} D1-SPNs. (E) There was a trend toward a decrease in *Foxp2*^{D1} D1-SPNs ($p = 0.08$). (F) ROIs used to quantify puncta for *Cdk7* in a similar fashion to *Ntn1*. Sample size (n) is the representative of the number of cells counted from each genotype. $n = 482$ cells, three mice (control, *Ntn1*); 403 cells, two mice (*Foxp1*^{D1}, *Ntn1*); 392 cells, two mice (*Foxp2*^{D1}, *Ntn1*); 536 cells, three mice (control, *Cdk7*); 636 cells, three mice (*Foxp1*^{D1}, *Cdk7*); and 626 cells, three mice

(*Foxp2*^{D1}, *Cdk7*). Scale bars represent 50 mM and images were taken at 20× magnification. A Mann-Whitney's U test was performed to assess statistical significance, *$p < 0.05$, ****$p < 0.0001$. All graphs are displayed as mean ± SEM.

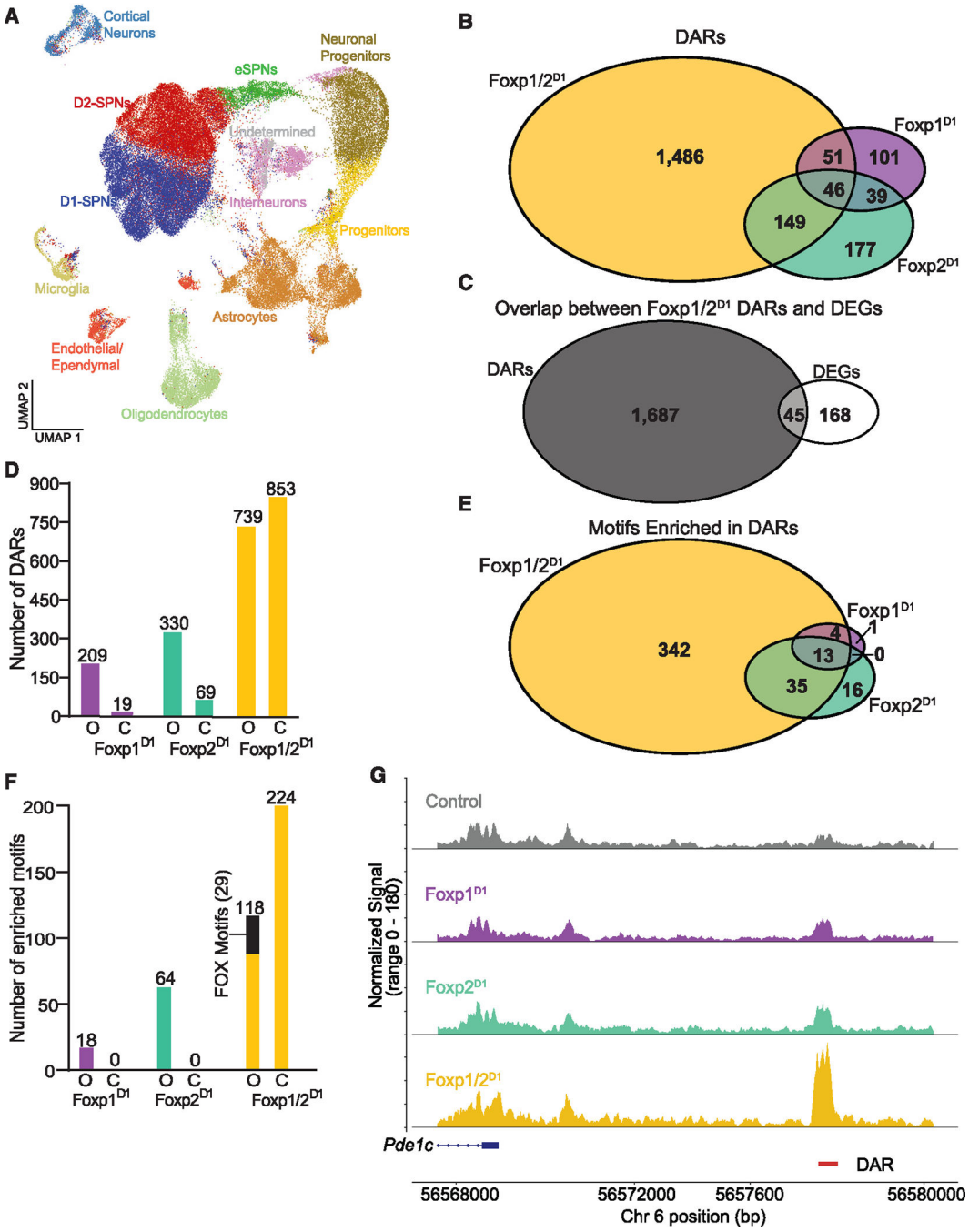

Figure 4. Loss of both Foxp1 and Foxp2 dysregulates chromatin state in D1-SPNs

(A) UMAP showing annotated cell types in snATAC-seq analysis. D1-SPNs were used for further DAR analysis. A region was called differentially accessible if it hadan adjusted *p* value <0.05 and a logFC > |0.1375|.

(B) Semi-scaled Venn diagram showing the number of unique and overlapping DARs within each condition. Overlap of DARs between conditions was assessed by a Fisher's exact test.

(C) Venn diagrams showing the overlap between DEGs and DARs in Foxp1/2^{D1} D1-SPNs. Overlap was assessed for significance by fold enrichment.

(D) Bar plot showing the number of more open or more closed regions in each knockout condition. Motifs enriched in the DARs of each knockout were identified.
(E) Semi-scaled Venn diagram showing the number of unique and overlapping motifs in each genotype. The significance of overlap of motifs was also assessedby a Fisher's exact test.
(F) Bar plot showing the number of motifs enriched within more open or more closed chromatin regions in each knockout condition. FOX motifs (GTAAACA) arehighlighted to indicate enrichment associated with more open regions.
(G) Trackfile for *Pde1c* with the differentially accessible region highlighted.

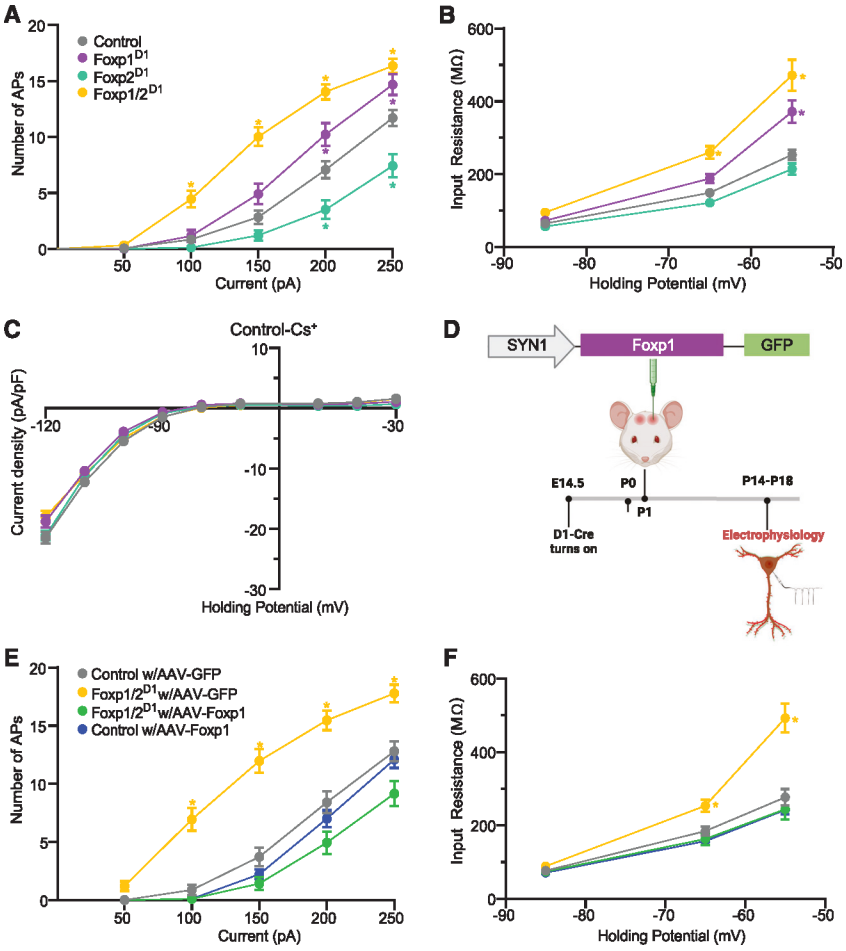

Figure 5. Loss of Foxp1 results in K_{Leak}-mediated hyperexcitability with amplification by further loss of *Foxp2*

(A) Number of action potentials recorded undercurrent-clamp conditions.

(B) Input resistance recorded from the same cells inthe same conditions.

(C) Contribution of K_{Leak} channels was determined by finding the difference in current density plots. Values recorded in presence of cesium (see Figure S4D) were subtracted from those recorded in its absence (see Figure S4C) with no significant differences observed.

(D) Schematic showing pAAV-hSYN-Foxp1-T2A-eGFP construct injected at P1. Dual presence of tdTomato and GFP was used to identify which neurons expressed the FOXP1 construct.

(E and F) (E) Current-clamp recordings to record number of action potentials and (F) input resistance. Repeated-measures two-way ANOVA with Holm-Sidak's *post hoc* test; only significant differences between knockouts and controls are shown. *$p < 0.05$ (A and B) n = 56 (control), 32 ($Foxp1^{D1}$), 40 ($Foxp2^{D1}$), and 41 ($Foxp1/2^{D1}$). (C) $n = 61$, 43, 38, and 41. (E and F) $n = 44$ (control with control virus), 34 ($Foxp1/2^{D1}$ with control virus), 32 ($Foxp1/2^{D1}$ with FOXP1 construct), and 19 (control with FOXP1 construct). All graphs are displayed as mean ± SEM.

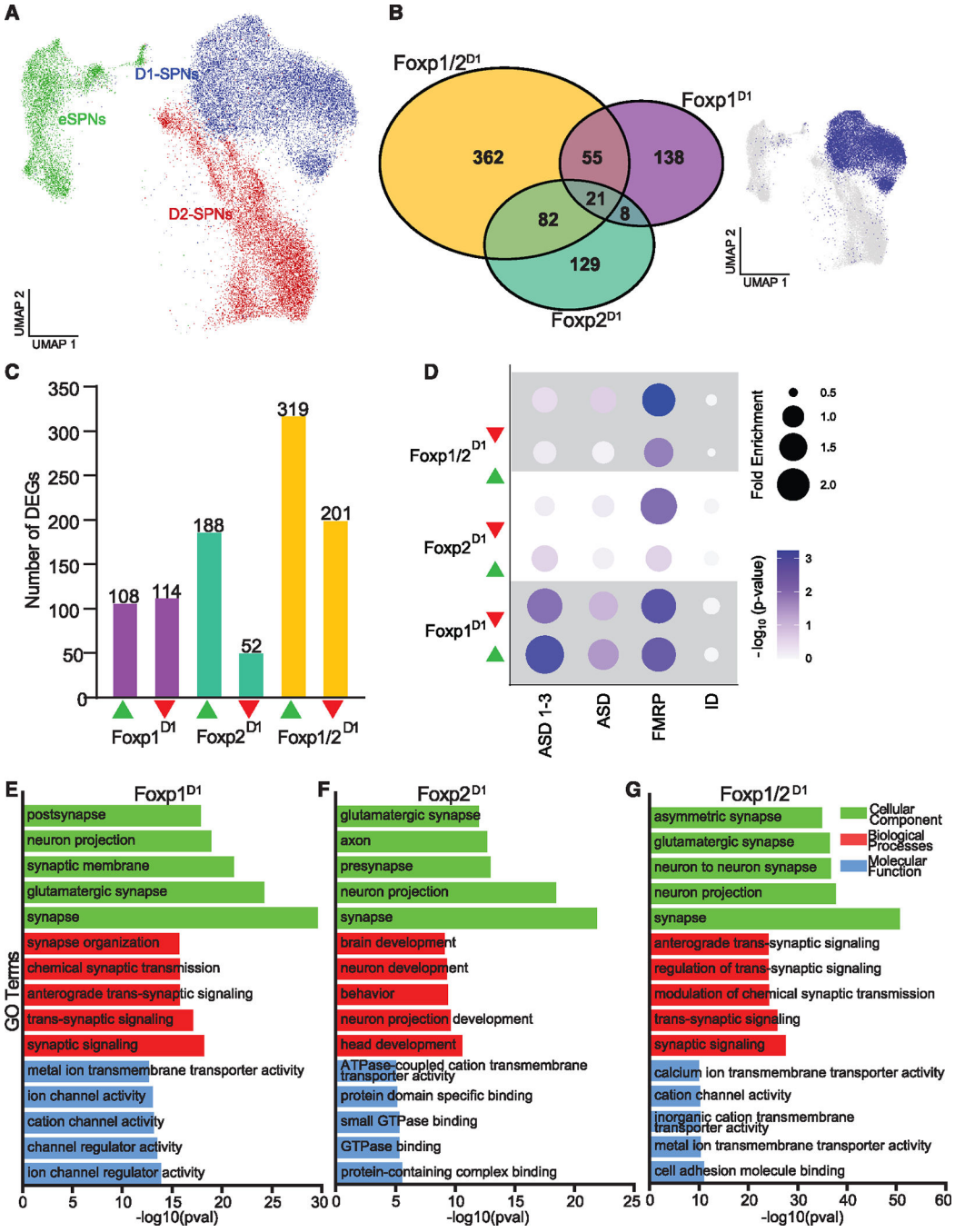

Figure 6. DEGs in adult SPNs have similar biological functions to those observed in juveniles

(A) UMAP of the neuron-only subset with colors indicating the cell types. D1-SPNs were used for further DEG analysis. Genes were called differentially expressed if they had an adjusted p value <0.05 and logFC > |0.25|.

(B) Semi-scaled Venn diagram showing number of unique and overlapping DEGs in each knockout condition in the D1-SPNs. Overlap of DEGs between conditions was assessed by a Fisher's exact test.

(C) Bar plots showing the number of up- and downregulated genes in each knockout condition.
(D) Bubble chart showing enrichment of DEGs from each knockout condition. The $-\log_{10}(p$ value) for each enrichment is indicated. ASD, SFARI ASD-risk genes; ASD 1–3, SFARI ASD-risk genes with scores of 1–3; FMRP, fragile X syndrome; ID, intellectual disability.
(E–G) Gene Ontology (GO) analysis of (E) $Foxp1^{D1}$, (F) $Foxp2^{D1}$, and (G) $Foxp1/2^{D1}$ DEGs reveals enrichment for terms associated with electrophysiological properties and synaptic properties.

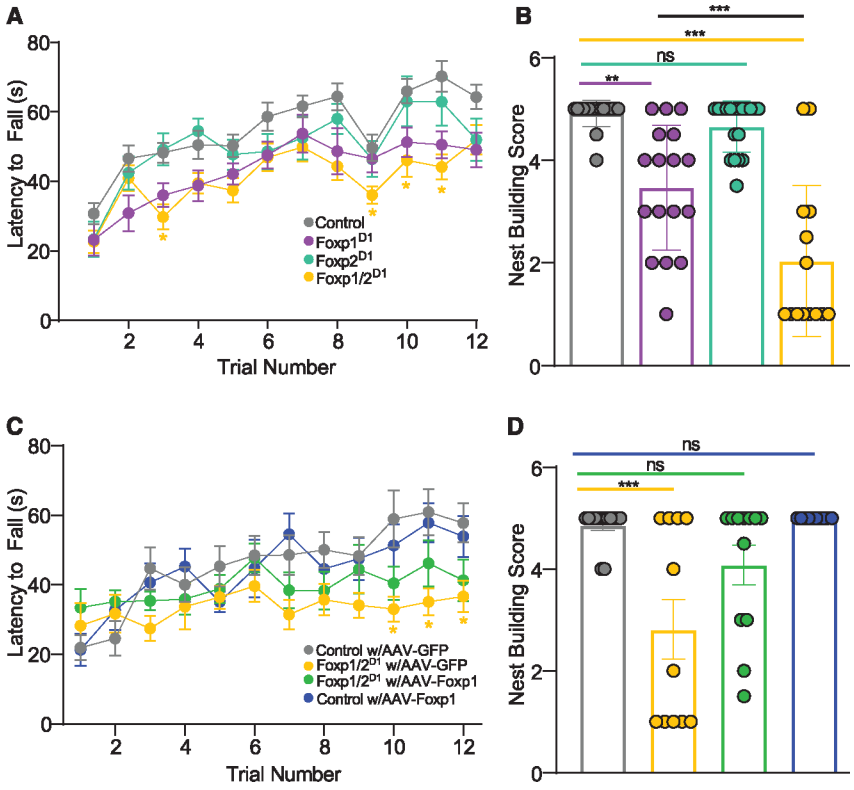

Figure 7. Loss of *Foxp1* and *Foxp2* results in impaired motor and social behavior

(A) Foxp1/2^{D1} mice show motor learning deficit as assessed by latency to fall using the rotarod paradigm.

(B) Nest-building quality was assessed after single housing for 24 h with Foxp1^{D1} showing impairment, and this is amplified in Foxp1/2^{D1}.

(C and D) AAV-mediated re-expression of *Foxp1* restored measures to baseline in rotarod (C) and nest building (D). (A and B) Behavior performed in control, Foxp1^{D1}, Foxp2^{D1}, and Foxp1/2^{D1}. (C and D) Performed in control or Foxp1/2^{D1} mice with either control AAV9-hSYN1-eGFP or pAAV-hSYN-Foxp1-T2A-eGFP construct. (A–D) Two-way ANOVA with Tukey's *post hoc* analysis used to determine significance. *$p < 0.05$, **$p < 0.01$, ***$p < 0.001$. n = 25 (control), 13 (Foxp1^{D1}), 14 (Foxp2^{D1}), and 16 (Foxp1/2^{D1}) for (A); $n = 15$, 13, 18, and 12 respectively for (B); and $n = 14$, 11, 12, and 10 respectively for (C) and (D). All graphs are displayed as mean ± SEM.

KEY RESOURCES TABLE

REAGENT or RESOURCE	SOURCE	IDENTIFIER
Antibodies		
Rabbit polyclonal anti-FOXPI	Spiteri et al.[54]	N/A
Goat anti-FOXP2 (N-terminal)	Santa Cruz	Cat#: sc-21069, RRID: AB_2107124
Rat anti-tdTomato	Kerafast	Cat# EST203; RRID: 2732803
Alexa Flour 488 Donkey Anti-Goat	Thermo Fisher	Cat#: A21206; RRID: AB_2534102
Alexa Flour 555 Donkey Anti-Rat	Thermo Fisher	Cat# A78945; RRID: AB_2910652
Alexa Flour 647 Donkey Anti-Rabbit IgG	Jackson ImmunoResearch Labs	Cat#: 711–605-152; RRID: AB_2492288
Bacterial and virus strains		
pAAV-hSYN-Foxp1-T2A-eGFP	Baylor College of Medicine Optogenetics and Viral Design/Expression Core	N/A
AAV9-hSyn-eGFP	Keaveney et al.[108]	Addgene Cat#: 50465-AAV9, RRID: Addgene_50465
Chemicals, peptides, and recombinant proteins		
TTX	Tocris	Cat#: 1078
ProLong Diamond Antifade Mountant	Thermo Fisher	Cat#: P36970
DAPI	Thermo Fisher	Cat#: D1306
CsCl	Sigma	Cat#: C4036–25G
Ultrapure BSA	Thermo Fisher	Cat#: AM2618
SUPERase-In RNase Inhibitor	Thermo Fisher	Cat#: AM2696
Hoechst	Santa Cruz Biotechnology	Cat# sc-394039
Blocker™ BSA	Thermo Scientific	Cat# 37525
Normal Donkey Serum	Millipore Sigma	Cat# S30–100ML
RNAscope ® probe Ms-Ntn1-mRNA	ACD Bio-techne	Cat# 407621
RNAscope ® probe Ms-Cdk7-C2-mRNA	ACD Bio-techne	Cat# 573911
RNAscope ® probe Ms-Tac1-C3	ACD Bio-techne	Cat# 410351
Critical commercial assays		
Chromium Single Cell 3' Reagent Kits v3	10X Genomics, Inc.	Cat#: 1000075
Chromium Single Cell 3' Reagent Kits v3.1	10X Genomics, Inc.	Cat#: 1000121
Chromium Single Cell ATAC 3' Reagent Kits v1.1	10X Genomics, Inc.	Cat#: 1000175
Chromium Single Cell ATAC 3' Reagent Kits v2	10X Genomics, Inc.	Cat#: 1000390
Nuclei Isolation Kit: Nuclei EZ Prep	Sigma	Cat#: NUC101–1KT
Nuclei Isolation Kit: Nuclei PURE Prep	Sigma	Cat#: NUC201–1KT
miRNeasy mini kit	QIAGEN	Cat#:217004
SSIII First-strand super mix	Life Technologies	Cat#: 18080400
iTaq Universal SYBR Green Supermix	Bio-Rad	Cat#: 172–5124
RNAscope ® Multiplex Flourescent Reagent Kit v2	ACD Bio-techne	Cat#: 323100

REAGENT or RESOURCE	SOURCE	IDENTIFIER
Deposited data		
Raw and Analyzed Data	This paper	GEO: GSE228826
Adult striatal single-cell RNA-seq dataset	Saunders et al.[72]	GEO: GSE116470
Experimental models: Organisms/strains		
Mouse: B6.FVB(Cg)-Tg(Drd1-cre)EY62GSat	MMRC	030989-UCD; RRID: MMRC_030989-UCD
Mouse: Drd1-tdTomato BAC Transgenic	Ade et al.[109]	N/A
Mouse: STOCK *Foxp1*$^{tm1.1Pwt}$/J	Jackson Laboratory	Strain#: 017699; RRID: IMSR_JAX:017699
Mouse: B6.Cg-*Foxp2*$^{tm1.1Sfis}$/CfreJ	Jackson Laboratory	Strain#: 026259; RRID: IMSR_JAX:026259
Oligonucleotides		
Drd1-Cre Forward genotyping primers: GCTATGGAGATGCTCCTGATGGAA	MMRC	N/A
Drd1-Cre Reverse genotyping primers: CGGCAAACGGACAGAAGCATT MMRRC	MMRC	N/A
Drd1-tdTomato Forward genotyping primers: CTTCTGAGGCGGAAAGAACC	Ade et al.[109]	N/A
Drd1-tdTomato Reverse genotyping primers: TTTCTGATTGAGAGCATTCG	Ade et al.[109]	N/A
Foxp1-flox Forward genotyping primers: CCAGGGATCAGAGATTACTGTAGC	Anderson et al.[18]	N/A
Foxp1-flox Reverse genotyping primers: CACCCTCTCCAAGTCTGCCTCAG	Anderson et al.[18]	N/A
Foxp2-flox Forward genotyping primers: ATGACCCACTTGCACATGCGA	This paper	N/A
Foxp2-flox Reverse genotyping primers: AGGGGTTTGAGGTAAGCTCTGT	This paper	N/A
Mus-Foxp1 F: CTACCGCTTCCATGGGAAAT	Anderson et al.[18]	N/A
Mus-Foxp1 R: ACTGTGGTTGGCTGTTGTCA	Anderson et al.[18]	N/A
Additional oligonucleotides listed in Table S3.	This paper	N/A
Software and algorithms		
CellRanger v3.0.2 (mkref, mkfastq, cont)	10X Genomics; Zheng et al.[110]	https://support.10xgenomics.com/single-cell-gene-expression/software/pipelines/3.0/what-is-cell-ranger
CellRanger ATAC v2.0.0 (mkref, mkfastq, count)	10X Genomics; Zheng et al.[110]	https://support.10xgenomics.com/single-cell-atac/software/pipelines/2.0/what-is-cell-ranger-atac
FastQC v0.11.5	Babraham Bioinformatics; Andrews[111]	https://www.bioinformatics.babraham.ac.uk/projects/fastqc/
CellBender	Fleming et al.[112]	https://cellbender.readthedocs.io/en/latest/
DoubletFinder	McGinnis et al.[113]	https://github.com/chris-mcginnis-ucsf/DoubletFinder
Seurat v4.3.0	Stuart et al.[114] Butler etal.[115]	https://satijalab.org/seurat/,https://github.com/satijalab/seurat
Harmony	Korsunsky et al.[116]	https://portals.broadinstitute.org/harmony/articles/quickstart.html

REAGENT or RESOURCE	SOURCE	IDENTIFIER
Signac v1.9.0	Stuart et al.[117]	https://stuartlab.org/signac/index.html
bcl2fastq v2.20.0	Illumina	https://support.illumina.com/sequencing/sequencing_software/bcl2fastq-conversion-software.html
ArchR v1.0.2	Granja et al.[118]	https://www.archrproject.com
BEDtools bamtobed v2.29.2	Quinlan and Hall[119]	https://bedtools.readthedocs.io/en/latest/
MACS2 callpeak	Zhang et al.[120]	https://github.com/macs3-project/MACS
MAST	Finak et al.[121]	https://github.com/RGLab/MAST/
Toppgene	Chen et al.[122]	https://toppgene.cchmc.org/
Deposited Code	This paper	https://doi.org/10.5281/zenodo.11094304